



HAL
open science

Origin of detrital fluxes in during the last climatic cycles the southeast Indian Ocean

Gilles Bareille, Francis Grousset, Monique Labracherie, Laurent Labeyrie,
Jean-Robert Petit

► **To cite this version:**

Gilles Bareille, Francis Grousset, Monique Labracherie, Laurent Labeyrie, Jean-Robert Petit. Origin of detrital fluxes in during the last climatic cycles the southeast Indian Ocean. *Paleoceanography*, 1994, 9 (6), pp.799-819. 10.1029/94PA01946 . hal-03587305

HAL Id: hal-03587305

<https://hal.science/hal-03587305>

Submitted on 24 Feb 2022

HAL is a multi-disciplinary open access archive for the deposit and dissemination of scientific research documents, whether they are published or not. The documents may come from teaching and research institutions in France or abroad, or from public or private research centers.

L'archive ouverte pluridisciplinaire **HAL**, est destinée au dépôt et à la diffusion de documents scientifiques de niveau recherche, publiés ou non, émanant des établissements d'enseignement et de recherche français ou étrangers, des laboratoires publics ou privés.

Origin of detrital fluxes in the southeast Indian Ocean during the last climatic cycles

Gilles Bareille, Francis E. Grousset, and Monique Labracherie

Département de Géologie et Océanographie, CNRS URA, Université de Bordeaux I, Talence, France

Laurent D. Labeyrie

Centre des Faibles Radioactivités, Laboratoire mixte CNRS-CEA, Gif-sur-Yvette, France

Jean-Robert Petit

Laboratoire de Glaciologie et Géophysique de l'Environnement, St Martin d'Heres, France

Abstract. Because of a close relationship between detrital flux variations and magnetic susceptibility (MS) flux (MS cm⁻³ of bulk sediment multiplied by the linear sedimentation rate) variations in the southeast Indian basin of the southern ocean, MS flux profiles have been used to examine the spatial and temporal detrital flux changes in this basin during the last climatic cycle. Results indicate a general increase in detrital material input during the coldest periods, suggesting a widespread phenomenon, at least on the basin scale. Mineralogical data, geochemical data, and ⁸⁷Sr/⁸⁶Sr isotopic ratios have been used to determine the origin and transport mechanisms responsible for increased detrital flux during glacial periods. Mineralogical and geochemical data show that these glacial "highs" are due to increases in both Kerguelen-Crozet volcanic and Antarctic detrital inputs. The ⁸⁷Sr/⁸⁶Sr isotopic composition of the >45- μ m fraction indicates that the Kerguelen-Crozet province contributes to at least 50% of the coarse particulate input to the west. This contribution decreases eastward to reach less than 10%. These tracers clearly indicate that the Crozet-Kerguelen province was a major source region of detrital in the western part of the basin during glacial times. In contrast, material of Antarctic origin is well represented in the whole basin (fine and coarse fractions). Because of the minor amount of coarse particles in the sediments, volcanic particles from Kerguelen and crustal particles from Antarctica have most probably been transported by the Antarctic bottom water current and/or the Circumpolar deepwater current during glacial periods as is the case today. Nevertheless, the presence of coarse particles even in low amount suggests also a transport by ice rafting (sea-ice and icebergs), originated from both Kerguelen and Antarctic sources. However, the relative importance of both hydrographic and ice-rafting modes of transport cannot be identified accurately with our data. During low sea level stands (glacial maximum periods), increasing instability and erosion of the continental platform and shallow plateaus could have resulted in a more efficient transfer of crustal and volcano-detrital material to the Southeast Indian basin. At the same time, extension of the grounded ice shelves over the continental margins and increase in the erosion rate of the Antarctic ice sheet could have induced a greater input of ice rafted detritus (IRD) to southern ocean basins. Enhancement of the circumpolar deepwater current strength might have also carried a more important flux of detrital material from Kerguelen. However, an increase in the bottom water flow is not necessarily required.

Introduction

The southern ocean strongly influences processes related to climate such as permanence of sea-ice cover, transfer of heat to the atmosphere, deepwater formation and global deep-ocean ventilation. Several box models, developed to gain a better

understanding the glacial decrease in atmospheric CO₂ concentrations, have predicted changes in southern ocean circulation [Toggweiler and Sarmiento, 1985; Wenk and Siegenthaler, 1985; Keir, 1988]. At present, water mass circulation in the southern ocean is controlled by (1) wind stress, which drives the eastward flowing Antarctic Circumpolar Current (ACC), (2) deep convection which renews bottom and deep waters, and (3) cyclonic subpolar gyres (Weddell, Ross, and East Indian) [Nowlin, 1991]. However, little is known about the southern ocean circulation response to both increasing sea-ice cover [Cooke, 1978; Cooke and

Copyright 1994 by the American Geophysical Union.

Paper number 94PA01946
0883-8305/94/94PA-01946\$10.00

Hays, 1982] and increasing atmospheric circulation (as assumed by *Petit et al.* [1981, 1990]), which occurred during glacial periods. Changes in bottom water velocity in the northern part of the Weddell Sea, inferred from sediment grain-size distribution [Fütterer *et al.*, 1988; Pudsey *et al.*, 1988; Pudsey, 1992], have been correlated with glacial-interglacial cycles. These results could indicate that bottom currents were weaker during glacial periods [Pudsey, 1992].

Recent preliminary results show a strong increase in detrital accumulation rates and enhancement of bulk low-field magnetic susceptibility (MS) signals in sediments from the southeast Indian sector of the southern ocean deposited during the coldest periods [Bareille, 1991]. These results raise questions about the origin, the mode of transport and the accumulation of these higher detrital inputs during glacial periods. One possible interpretation is that they represent changes in the surface water circulation, initiating greater important input of ice-rafted detritus (IRD) [Cooke, 1978; Cooke and Hays, 1982; Labeyrie *et al.*, 1986]. This process has clearly been identified in the northern Atlantic Ocean during the last glacial (Heinrich layers) [Bond *et al.*, 1992; Grousset *et al.*, 1993]. A second hypothesis is that they represent changes in bottom water circulation; enhancement of oceanic circulation would be responsible for an important transfer of detrital material to deep basins, as observed in the northern Atlantic by Poutiers and Gonthier [1978]. Finally, a third possibility would be a large input of dust particles due to increased intensity of atmospheric circulation and to higher aridity on continents [Rea *et al.*, 1986; Kukla, 1987; Kukla *et al.*, 1988; Hovan *et al.*, 1989; Kukla and Han, 1989; Clemens and Prell, 1990; Petit *et al.*, 1990]. Considering the visual

similarity between the Vostok dust flux record and the MS record obtained by Kent [1982] in the Indian Ocean (core RC11-120; 79°52'E, 43°21'S), Petit *et al.* [1990] suggested that the major MS peaks in this marine core are partly due to continental dust input. However, Grousset *et al.* [1992] showed that Last Glacial Maximum dusts found in East Antarctica at Dome C came mostly from Argentine loesses (Patagonian), a source region which is remote from the southeast Indian Ocean. In addition, Duce *et al.* [1991] found modern dust fluxes in the southern ocean to be low to nonexistent. Thus, although a direct relationship between aeolian inputs and MS signal was identified in the northern hemisphere [Robinson, 1986a, b; Bloemendal and De Menocal, 1989], such a relationship still needs to be demonstrated for the southern ocean. Independent information on the origin of detrital materials is needed to define both the specific source of detrital minerals (magnetic and nonmagnetic) and the major transport mechanism (aeolian or hydrographic). In order to understand better the spatial and temporal distributions of the detrital flux increases, and their origin and implication for the paleoceanographic history of the southern hemisphere, we (1) demonstrated that MS measurements can be used as a tracer of oceanic detrital inputs in the Indian sector of the southern ocean during the last climatic cycle, (2) identified the origins and the transport mechanisms of detrital material, using mineralogical, geochemical and isotopic data.

Analytical Methods and Results

Box cores and piston cores (Figure 1) studied here were recovered from the Indian sector of the southern ocean

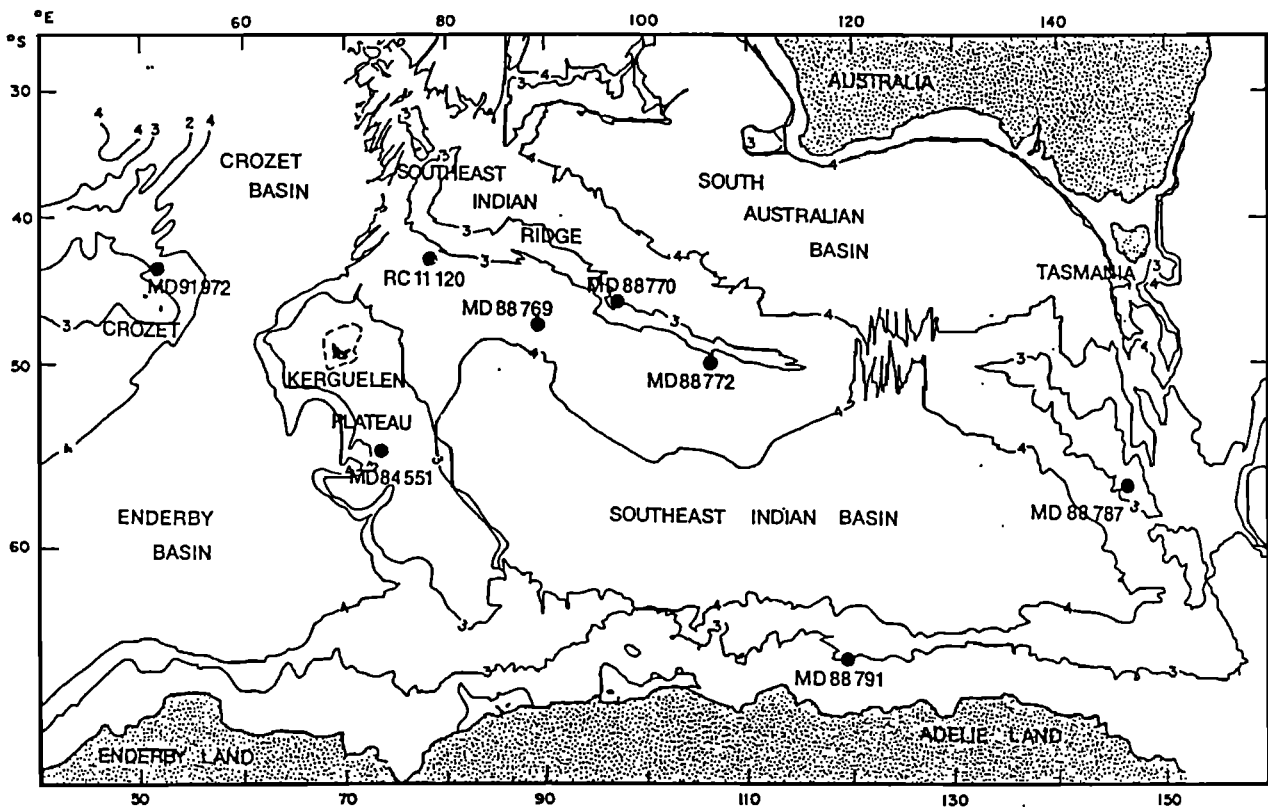


Figure 1. Downcore locations in the southeast Indian basin of the southern ocean.

(between Kerguelen, South Australia, and Antarctica), during oceanic cruises supported by French PNEDC (national program of climate dynamic studies). Box cores, previously studied for biogenic silica accumulation by *Bareille et al.* [1991], were examined to evaluate modern variability in detrital sources and input to the southeast Indian basin. In order to characterize the spatial and temporal changes in detrital fluxes during the last climatic cycle, we chose to focus on eight cores selected to provide a complete view of the southeast Indian basin, according to the modern detrital dispersal scheme (Figure 1; Table 1). Five of the cores come from the southeast Indian Ridge, one comes from the northeast flank of the Crozet Plateau, and one comes from the western margin of the Kerguelen Plateau. The most southern core is located on the Antarctic continental slope, near Adélie Land. Most of them are located on shallow ridges or seamounts and were chosen to represent the main sedimentary conditions of the Indian sector of the southern ocean. We also examined the Lamont core RC11-120, located on the southeast Indian Ridge, which provides a continuous record of climatic change for the past 250,000 years [Martinson et al., 1987]. In all the cores located north of the present-day Antarctic Polar Front Zone, carbonate oozes alternate with siliceous oozes. These alternations represent northward and southward migration of the Antarctic Polar Front zone (APFZ) in response to glacial/interglacial cycles. South of the Antarctic Polar Front Zone, siliceous oozes overlie and

interfinger with glaciomarine sediments which consist of silty clay or clayey silt with varying amounts of biogenic silica. These alternations might be the result of the northward and southward glacial advances and retreats. Stratigraphic framework was provided by *N. pachyderma* (sin.) $\delta^{18}\text{O}$ records, carbonate [Howard and Prell, 1992] and opal [Mortlock et al., 1991] content variations, and by biostratigraphic tracers, that is, variations in the abundance of the radiolaria *Cycladophora davisiana* [Hays et al., 1976] and the last abundant appearance of the diatom *Hemidiscus karsteni* [Burckle et al., 1978]. Oxygen isotopic ratios were measured at the C.F.R. (Gif-sur-Yvette) on planktonic foraminifera tests of *Neoglobobulimina pachyderma* (sin.) ($\delta^{18}\text{O}$ versus Pee Dee Belemnites standard) in four of the cores. Two cores lie within the Antarctic Polar Front Zone (MD 88-769 and MD 88-770) while two cores are located most southerly within Antarctic waters (MD 84-551 and MD 88-787). The *N. pachyderma* (sin.) $\delta^{18}\text{O}$ record of cores MD 88-769, MD 88-770, and MD 84-551 was previously published [Labracherie et al., 1989; Bareille, 1991; Pichon et al., 1992]. The *N. pachyderma* (sin.) $\delta^{18}\text{O}$ records cannot be directly compared to the "standard" oxygen isotope signal given by Imbrie et al. [1984], Labeyrie et al. [1987], and Martinson et al. [1987] because of important changes in surface water temperature and salinity, and meltwater discharges [Labeyrie et al., 1986]; however, the main isotopic events reported by Martinson et al. [1987] can be recognized in our cores. All the stratigraphic parameters

Table 1. Samples and Sr Isotopic Composition

Samples	Sources	Latitude	Longitude	Depth, m	$^{87}\text{Sr}/^{86}\text{Sr}$ ($\pm 2\text{sig.} \times 10^{-6}$)	1000/Sr
<i>Southeast Indian Basin Cores (Samples From Isotopic Stage 2)</i>						
RC11-120		43°31' S	79°52' E	3135	n. d.	-
MD 91-972	1	44°27' S	51°33' E		0.704287 (± 16)	1.34
MD 88-769	1	46°04' S	90°07' E	3420	0.705616 (± 17)	2.03
MD 88-770		46°01' S	96°28' E	3290	n. d.	-
MD 88-772	1	50°01' S	104°54' E	3240	0.706964 (± 26)	1.92
MD 84-551	1	55°00' S	73°20' E	2230	0.705941 (± 32)	1.4
MD 88-787	1	56°23' S	145°18' E	3020	0.712442 (± 11)	3.76
MD 88-791	1	64°40' S	119°28' E	3150	0.731746 (± 12)	5.02
<i>Potential Volcanic Detrital Sources</i>						
Kerguelen Island	1	49° S	70° E		0.705675 (± 10)	2.14
Kerguelen Island	2	49° S	70° E		0.70463-0.70767	0.65-2.7
Crozet Island	3	46° S	50° E		0.70411	-
Tristan Da Cunha	4	37° S	12° W		0.70504-0.70517	0.71-1.8
Bouvet Island	4	54° S	3° E		0.70365-0.70376	1.9-3.28
SIR	2	28°-41° S	70°-80° E	basaltes	0.70288-0.70411	12.2-4.1
SSI	5	54°-62° S	25°-35° W		0.70376-0.70423	5.1-9.1
<i>Antarctic Potential Detrital Sources</i>						
Enderby Land	6	65° S	50° E	rocks	0.7134-0.7372	7.8-22.3
KR 8817	7	66° S	141° E	180	0.736836 (± 42)	n.d.
Terre Adélie	7	67° S	140° E	moraines	0.760616 (± 24)	14.8
<i>Potential Dust and Loess Sources</i>						
Argentina	7	35°-38° S	58°-62° W		0.706599 (± 38)	3.54
South Africa	7	23°-29° S	15°-20° E		0.71689- 0.7464	n.d.
Australia	7	18°-31° S	124°-142° E		0.72182-0.76336	5.0

Accuracy of the $^{87}\text{Sr}/^{86}\text{Sr}$ isotopic ratio measurements is expressed as ($\pm 2\text{sig.} \times 10^{-6}$), which we tried to keep below 40×10^{-6} . Sources: 1, this work; 2, Dosso et al. [1979] and Dosso et al. [1988]; 3, Dupré and Allègre [1983]; 4, O'Nions and Pankhurst [1974]; 5, Hawkesworth et al. [1977]; 6, De Paolo et al. [1982]; 7, Grousset et al. [1992]; n. d.= not determined; SIR: Southeast Indian Ridge; SSI: South Sandwich Island.

($\delta^{18}\text{O}$ records, carbonate and opal content variations, and variations in the abundance of the radiolaria *Cycladophora davisiana*) were reported and calibrated to those of core RC11-120. For this core, reference ages were derived from the $\delta^{18}\text{O}$ record by detailed correlation of stages with the SPECMAP-stacked, $\delta^{18}\text{O}$ signal [Imbrie et al., 1984; Martinson et al., 1987].

Magnetic Susceptibility: Records of Detrital Input Changes

Common detrital sources of magnetization in sediments are lithogenic fragments from continental and submarine erosion and volcanic and cosmic input. In contrast to biogenic tests, calcite and quartz, which all have a very low or negative MS, iron-rich clay minerals [Pouiters, 1975], goethite [Robinson, 1986b], titanite and iron-rich magnetite [Pouiters and Gonthier, 1978], and iron sulfides such as pyrrhotite or greigite [Pouiters, 1975], are potential sources of high MS signal. The integrated MS depends on (1) the average susceptibility of individual particles, (2) the relative volume of both low (or negative) MS and high MS particles, and (3) the sediment porosity. Consequently, bulk sediment MS records varying inputs of material derived from continental crust or from mantle origin within a biogenic matrix [Pouiters, 1975; Pouiters and Gonthier, 1978]. Thus changes in detrital flux to the sediments, which can introduce large changes in the amount of MS particles, would be recorded in the MS signal. Continuous measurements of low-field magnetic susceptibility (MS) were taken on all core samples with a pass-through Bartington magnetometer. This instrument integrates the sediment section within the coil (12.5-cm diameter). The resolution of the signal is only about 5-10 cm. The great advantage of the use of MS records is that, in contrast to conventional sedimentologic methods, it is a nondestructive, extremely rapid method that provides semi quantitative lithostratigraphy.

We checked the relationship between MS and detrital inputs in the southeast Indian Basin. The total amount of detrital material was determined by subtracting from 100% both carbonate and opal contents (Appendix A, example of core data downloaded into the NGDC database). Carbonate content was obtained by the gasometric method with a $\pm 2\%$ accuracy. Opal content was measured by X ray diffraction [Bareille et al., 1990] and chemical [Mortlock and Froelich, 1989] methods. Both approaches gave similar results (G. Bareille, unpublished results, 1994), but there must be a year we used those from the chemical method for calculation because of their better accuracy ($\pm 2\%$ compared to $\pm 10\%$ with X ray diffraction). Thus, detrital percentage were estimated to $\pm 4\%$. MS and detrital data were expressed as magnetic susceptibility fluxes and detrital fluxes (in c.g.s. $10^{-6} \text{ cm}^{-2} \text{ kyr}^{-1}$ and $\text{g cm}^{-2} \text{ kyr}^{-1}$, respectively) by multiplying both MS cm^{-3} of sediment and g of detrital cm^{-3} of sediment by the sediment accumulation rates (cm kyr^{-1}) derived from the stratigraphic timescale. The dry bulk sediment density (DBD) was obtained for each sample by the water loss technique from a constant wet-volume sampling. Values range from 0.8 g cm^{-3} in carbonate oozes and glacio-marine sediments to 0.3 g cm^{-3} in siliceous oozes. Accuracy on DBD measurement is $\pm 5\%$. Assuming a precision of about 10% on linear sedimentation

rates (LSR), we calculated an error around 60% and 20% on minimum and maximum detrital fluxes, respectively. Nevertheless, core logging sensors provide high-precision MS measurements; therefore we can expect a precision lower than 20% on MS fluxes.

As a first approximation, the geographic distribution of MS flux (Figure 2a) displays the same distribution pattern as that of detrital flux (Figure 2b) during the Holocene epoch, suggesting that MS can be considered as a good proxy of detrital input. The geographic pattern of both MS flux and detrital flux (Figures 2a and 2b) clearly shows three main decreasing gradients during the Holocene period, one from the Kerguelen and Crozet islands and plateaus to the east, one from the Antarctic continent to the north, and the last one from Tasmania to the south. Two of the potential lithogenic sources are characterized by lithogenic material with relatively high MS values, one of mantle-derived origin, the volcanogenic province of Kerguelen, and the other of crustal origin, the Antarctic province. The Australian province provides smaller amount of magnetic particles. Near the Kerguelen Plateau, MS flux values (more than $5 \times 10^{-6} \text{ c.g.s. cm}^{-2} \text{ kyr}^{-1}$) are higher than along the Antarctic continental slope (less than $1 \times 10^{-6} \text{ c.g.s. cm}^{-2} \text{ kyr}^{-1}$) (Figure 2a) although detrital fluxes are of similar amplitude close to the two areas ($0.8\text{-}1.5 \text{ g cm}^{-2} \text{ kyr}^{-1}$) (Figure 2b). This observation supposes that the Antarctic province provides a detrital stock with globally less high-MS minerals compared to the volcanogenic province (Kerguelen). Indeed, difference in the amount of high-magnetic particles relative to the total stock of detrital particles from both sources result in variable detrital flux/MS flux ratios close to each lithogenic domain (2 close to the volcanic source, 1 near the Antarctic province, and about 0.1 close to the Australian province).

To verify that MS changes actually record changes in detrital inputs during the past 200 kyr, we examined both detrital flux changes and MS flux changes in two cores, one from the southeast Indian Ridge (MD 88-769) close to the volcanogenic source of Kerguelen, and the other from the Antarctic continental slope (MD 88-791). Unfortunately, we were not able to test this approach for the Australian province because no good core was available there. We found a strong correlation between the two flux records ($R=0.89$ and $R=0.91$ for MD 88-791 and for MD 88-769, respectively), both around the volcanic and Antarctic sources (Figure 3), confirming the usefulness of MS flux as a proxy of lithogenic flux changes in the basin. Taking into account the advantage of MS (rapidity and nondestructiveness, and its close relationship to the detrital inputs in the basin studied), we examined changes in detrital flux by using MS profiles. Continuous down-core records of MS from the southern Indian Ocean, expressed as magnetic material accumulation rates, were obtained from seven cores (Figures 4a and 4b). We used MS flux instead of bulk MS signals because this method gives similarly quantitative and better comparable data. Significant low-frequency MS flux variations are found in all the cores, both in the Subantarctic and Antarctic regions. These fluctuations are similar to the one observed by Petit et al. [1990] for deep-sea core RC 11-120 (Figure 4a). MS flux were systematically higher during coldest periods (Figures 4a and 4b), suggesting a global increase in detrital material input during isotopic

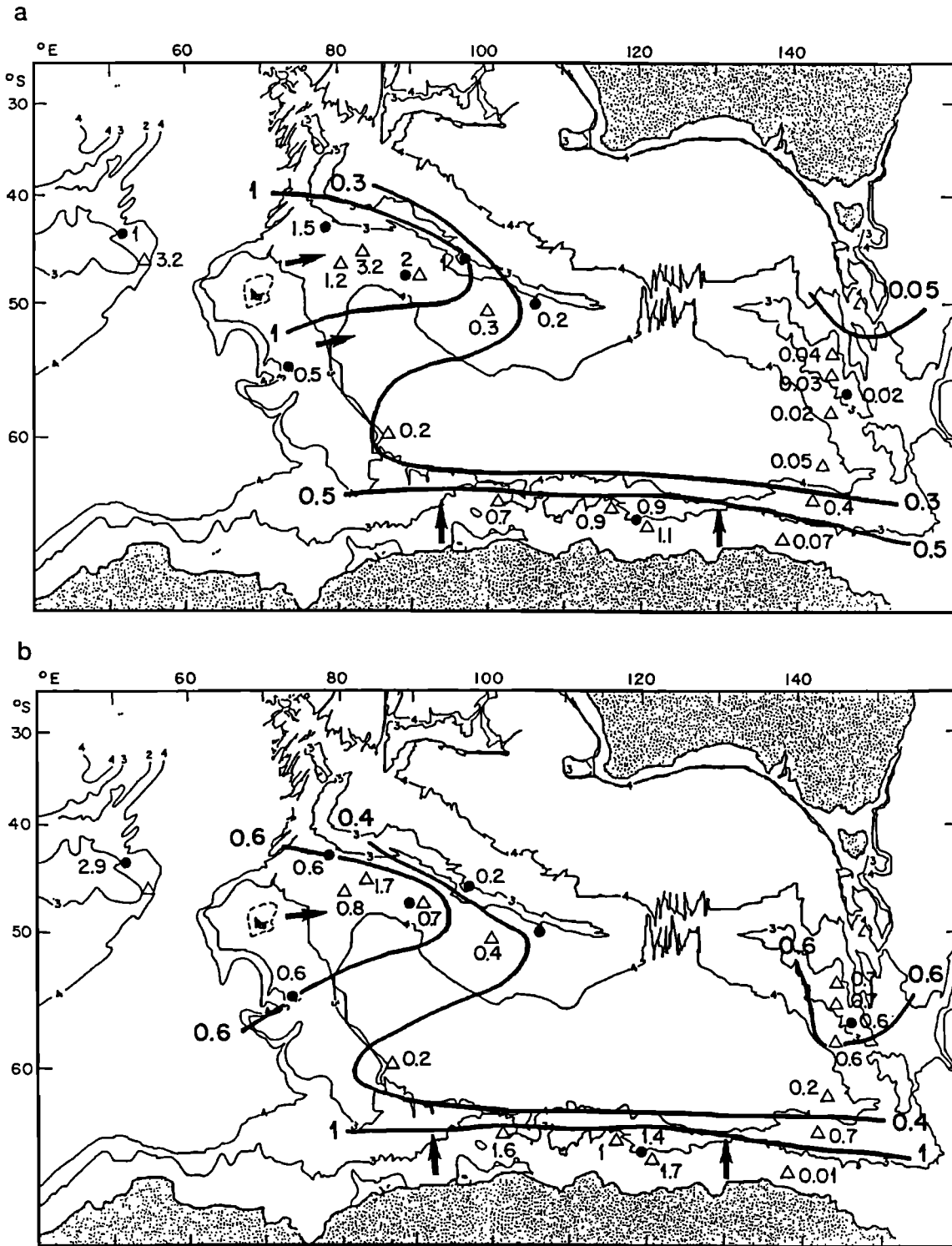


Figure 2. (a) Magnetic susceptibility flux and (b) detrital flux distribution during the Holocene in the Southeast Indian basin; isoflux line are in $\text{g cm}^{-2} \text{kyr}^{-1}$ and $10^{-6} \text{c.g.s. cm}^{-2} \text{kyr}^{-1}$, respectively. Arrows show the main sources and transport direction of the detrital and magnetic material.

stages 2, 4, and 6, at least on the scale of the basin. On the other hand, the observed flux gradients during the Holocene from Kerguelen Plateau and from Antarctic continent (Figure 2), are also well defined during oxygen isotopic stages 2, 4,

and 6 (Figures 5a, 5b, and 5c). There is no evidence of any shift in latitude for the west-to-east gradient, clearly suggesting the same dispersal mode for lithogenic material during glacial times and the Holocene, at least in the western

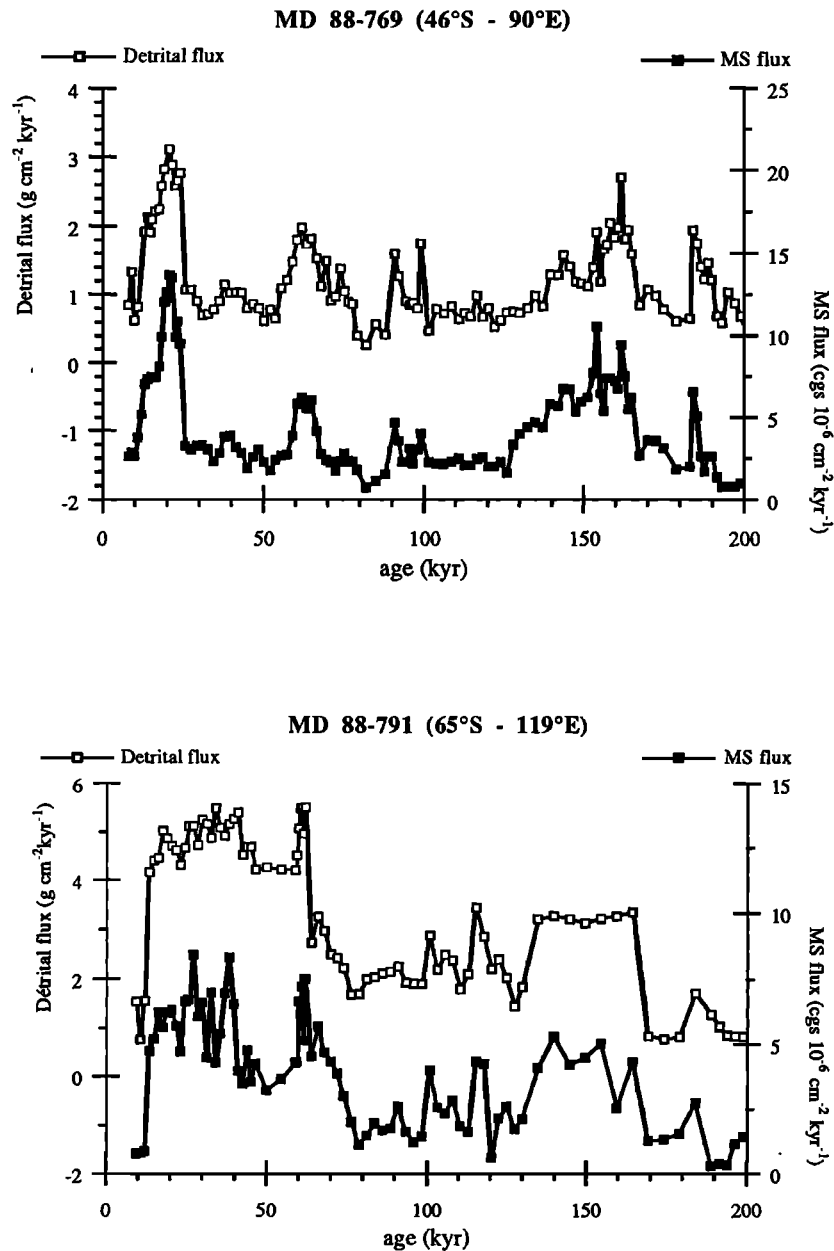


Figure 3. Comparison between detrital flux changes and MS flux changes in two cores, one close to the Kerguelen detrital source (MD 88-769 - 46°S-90°E) and one on the Antarctic continental slope (MD 88-791 - 64.5°S-119.5°E), during the 200,000 last years. Detrital flux and MS flux are expressed in $\text{g cm}^{-2} \text{kyr}^{-1}$ and in $10^{-6} \text{ c.g.s. cm}^{-2} \text{kyr}^{-1}$, respectively.

part of the basin (Figure 5). However, we do not have enough cores in the eastern part of the basin to comment on glacial input changes from the Australian source, even though lowest detrital fluxes are found in this part of the basin during glacial periods (core MD 88-787). Considering MS flux as a first order approach, we observe an increase in terrigenous flux by a factor 4-10 during the last glacial maximum. Several relatively high-frequency MS flux peaks of limited amplitude are observed in most of the cores, in addition to the general variation. In core MD 91-972, located in the northeastern part

of the Crozet volcanic Island (Figure 1), several disproportionately high MS flux peaks (Figure 4b) are associated with volcanic-ash-rich sediments which probably result from local input of Crozet volcanic material. However, both low-resolution analysis of the detrital fraction and inaccuracy of the age control reduce the use of these secondary peaks, even though they could have an important paleo-hydrologic significance. A better evaluation of the origin and importance of such events would require high-resolution analysis of the terrigenous fraction. In any case the strong connection

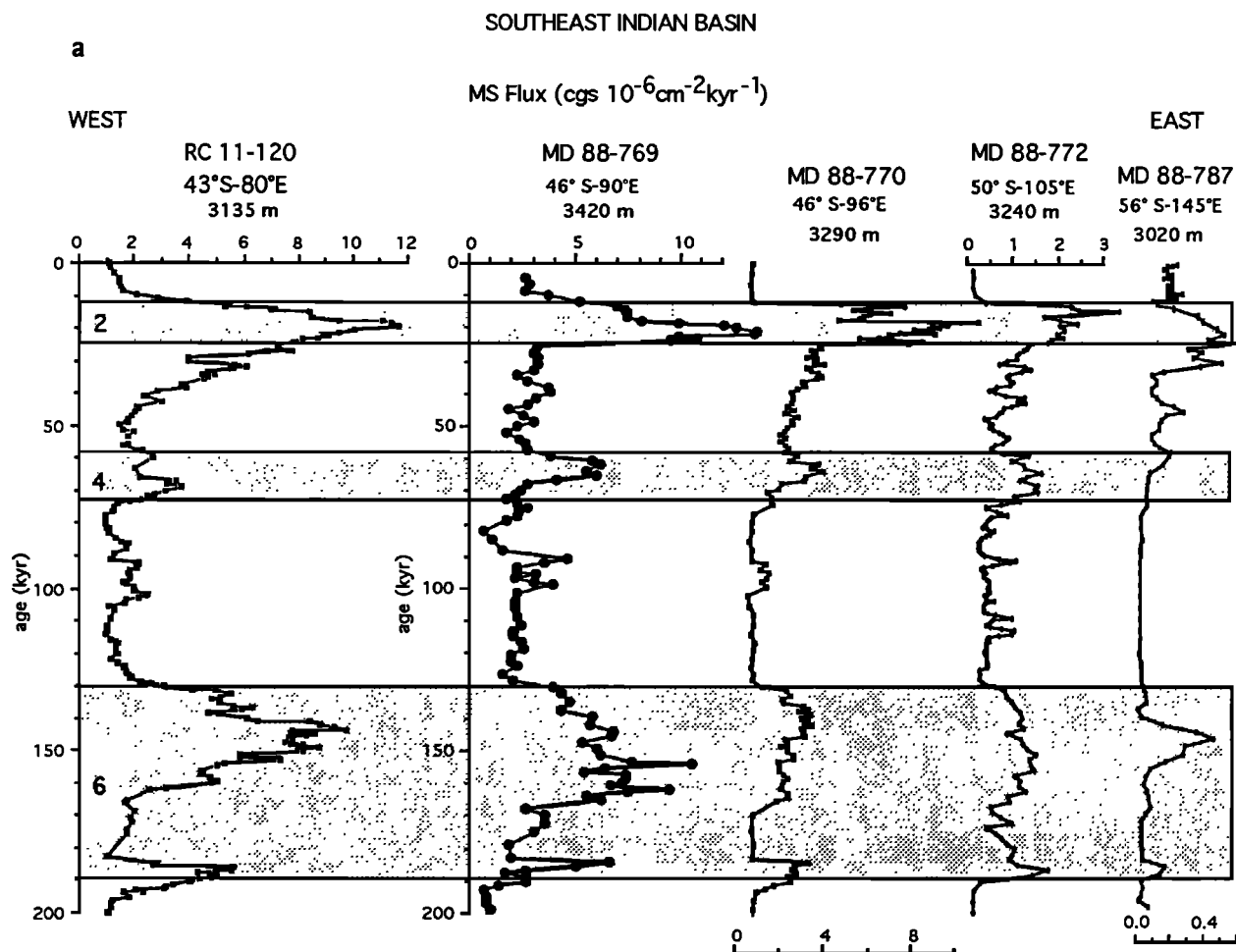


Figure 4. Downcore magnetic susceptibility flux profiles in the southeast Indian Ocean: (a) on an west-east transect between Kerguelen Plateau and South Tasmania; RC 11-120 MS flux has been calculated using MS values given by *Kent* [1982] and age given by *Martinson et al.* [1987]; (b) on the northeast flank of the Crozet Island, on the southwest part of the Kerguelen Plateau, and on the Antarctic continental slope. All the MS flux are expressed in 10^{-6} c.g.s. $\text{cm}^{-2} \text{kyr}^{-1}$. Glacial isotopic stages are represented by shaded bands.

between MS flux increase and cold isotopic events as recorded by both $\delta^{18}\text{O}$ and *C. davisiana* records suggests a paleoclimatic control on detrital input. Such a climatic control on MS signals was previously indicated by *Robinson* [1986a, b] in the North Atlantic, *Bloemendal et al.* [1988] in the eastern equatorial Atlantic, and *DeMenocal et al.* [1991] in the Arabian sea. Although MS changes were attributed to dilution of pelagic carbonate flux by ice-rafted detritus discharges during glacial periods [*Heinrich*, 1988; *Robinson*, 1986a, b; *Grousset et al.*, 1993] in the North Atlantic, these changes have been induced by higher eolian inputs during glacial in the eastern equatorial Atlantic and the Arabian sea [*Bloemendal et al.*, 1988; *DeMenocal et al.*, 1991].

Detrital Mineralogy Changes

X ray diffraction (XRD) analyses were performed on the carbonate-free fraction to determine relative amounts of the major minerals: clays, feldspars, quartz. Quartz content was calculated using a calibration curve. Because feldspar cannot be

easily quantified, we used XRD quartz/feldspar peak area ratio and the quartz percentage to estimate relative changes in the amount of feldspar. Individual clay minerals were identified by their basal reflections [*Biscaye*, 1965] on the same XRD diagram. A qualitative analysis was also carried out by mean of microscopic observations on smear slides. According to XRD and microscopic investigations, terrigenous material from the western part of the basin consists of alkali feldspar, iron-rich smectite, volcanic minerals (Ti-rich and aegyrinic augite) and glasses, and minor amounts of quartz and accessory minerals. The clay fraction is mainly composed of smectite to the West and along the South flank of the southeast Indian ridge. An important part of these minerals could provide a high-specific MS signal (volcanic glasses, iron-rich smectite, Ti-rich minerals). Indeed, recent studies indicated that since the Eocene, the continuous fallout of volcanic ash from explosive volcanism on the Kerguelen Archipelago has been an essential source of magnetic particles to the Kerguelen plateau and probably to the south Indian Basin [*Heider et al.*, 1993].

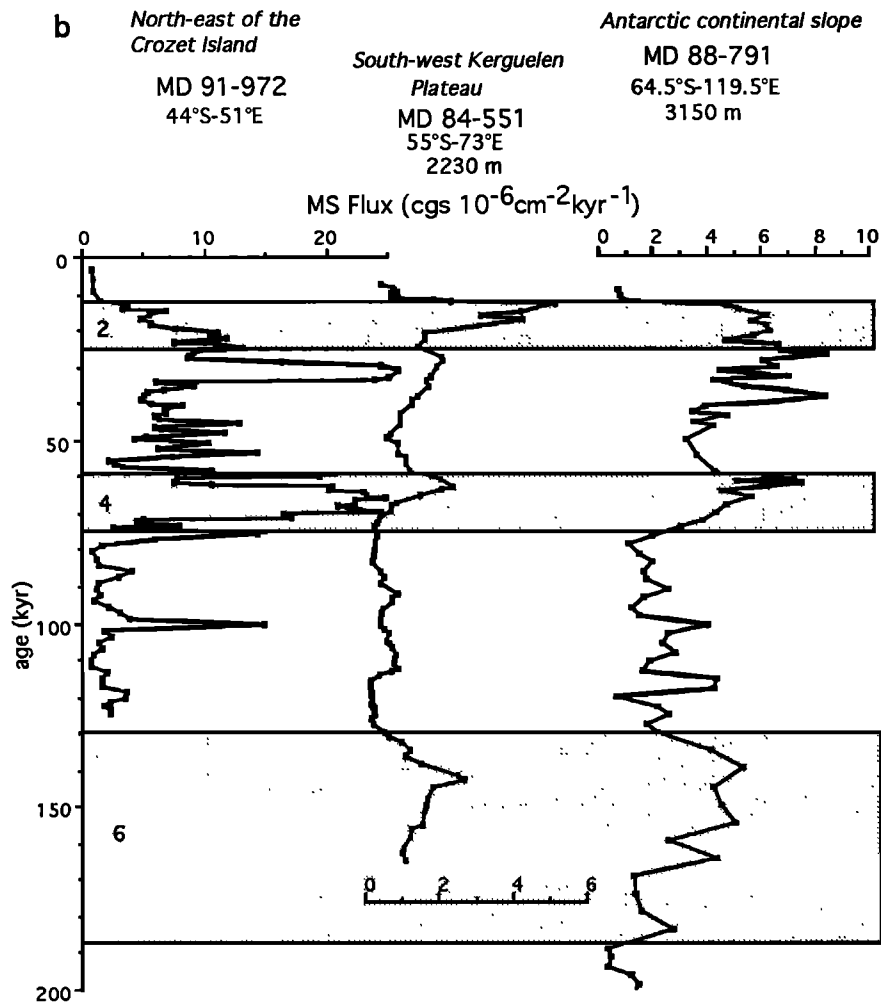


Figure 4. (continued)

These magnetic particles, which were identified as titanomagnetites included in volcanic glass, or as individual crystals [Heider *et al.*, 1993], could explain the high MS found in the western part of the basin. In contrast, the lithogenic assemblage found close to Antarctica is mainly characterized by large amount of quartz with relatively low MS, but contains important amount of others minerals (felspar, illite, chlorite, mica, smectite, blue-green hornblende, and alumino-silicate type andalousite) with variably high MS [Poutiers, 1975]. In this part of the basin, the clay fraction is dominated by high proportions of illite and chlorite, which represent glacially derived clay minerals.

Microscopic observation and XRD of the carbonate-free fraction were made on cores MD 88-769 and MD 88-770 from southeastern Indian ridge (Figure 6) because higher detrital fluxes at these sites suggested a more important contribution of source materials during glacial periods. The detrital mineralogy observed during the Holocene is dominated by various silicate materials, mostly clay minerals and feldspars (mostly plagioclases), and then by quartz, volcanic minerals (Ti-rich and aegyrinic augite) and glasses. The same composition is observed throughout the last climatic cycle. Mineralogic analysis made in few samples of Lamont core

RC11-120 are consistent with cores MD 88-769 and MD 88-770 records. Because most of the feldspars are commonly alkali plagioclases and smectites are rather iron-rich in this western part of the basin, an important volcanic contribution is suggested both during glacial and interglacial periods. Furthermore, between Kerguelen and 100°E, the glacial detrital fraction $>45 \mu\text{m}$ is mainly constituted by minerals with a volcano-alkalin facies (basaltic hornblende, Ti-rich and aegyrinic augite, glass), which is a typical Kerguelen and Crozet signature (J. C. Pons, personal communication, 1992). However, the presence of minerals of crustal origin (quartz, illite and chlorite, blue-green hornblende), clearly demonstrates an Antarctic contribution to this part of the basin during the last glacial maximum. Smear slide examination of the detrital fraction from the eastern part of the basin indicates that minerals are mainly derived from the Antarctic continent: abundant quartz, chlorite, blue-green hornblende, alumino-silicate andalousite type (J. C. Pons, personal communication, 1992). The high smectite proportion probably reveals an associated volcanogenic origin. This result suggests that the influence of the volcanic source was much more limited in the eastern part both during glacial and interglacial times. Quartz content, relative felspar content and

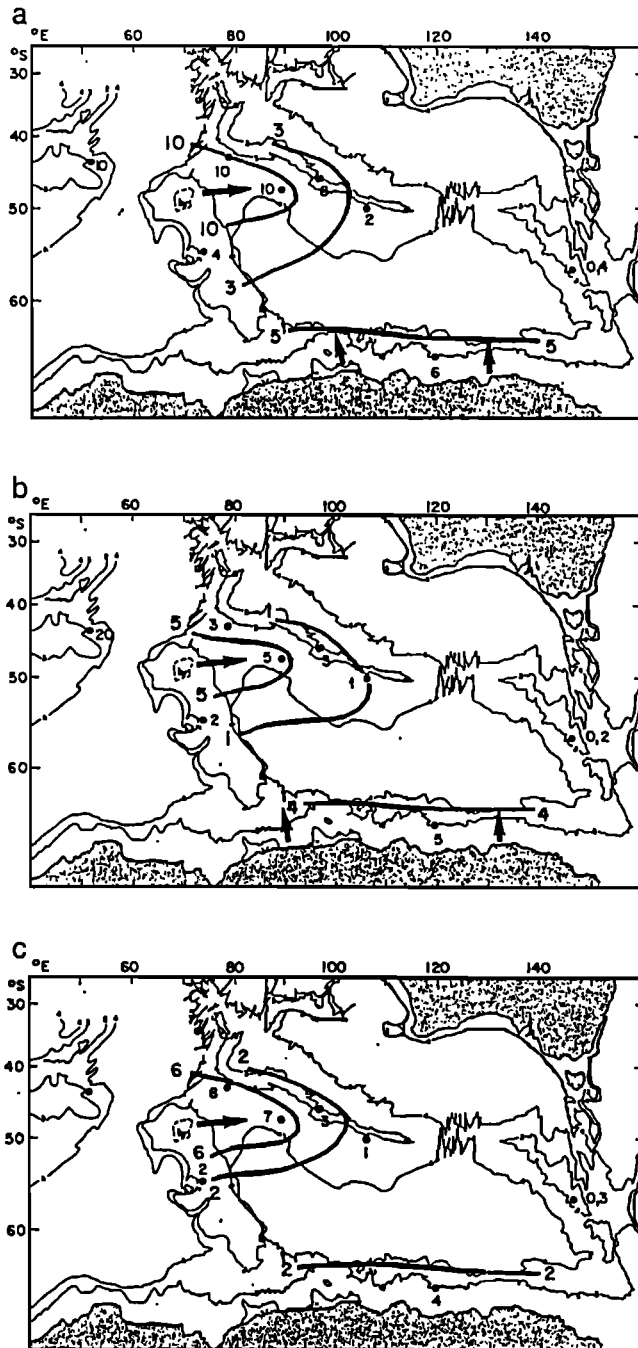


Figure 5. Magnetic susceptibility flux distribution during isotopic stages (a) 2, (b) 4, and (c) 6 in the southeast Indian Ocean.

the remaining terrigenous fraction ("other detrital") including clay minerals (smectite, illite and chlorite), volcanic derived minerals, and accessory minerals, were expressed as mass accumulation rates in $\text{g cm}^{-2} \text{kyr}^{-1}$. Large increases in feldspar flux (by a 20-fold factor), in quartz flux (by a 10-fold factor) and in other detrital particles flux (by a 10-fold factor) characterize the last glacial period (Figure 6). Feldspar flux (Figure 6b) clearly shows an eastward decreasing trend, whereas the "other detrital particles" flux (Figure 6c) display

an inverse tendency, with a low eastward increasing gradient. The quartz flux (Figure 6a) seems to be constant. These trends could correspond to a transport by size from Kerguelen, with rapid accumulation of coarse and high-density particles like feldspars close to the source. Clay minerals, which are much finer and then can be transported far away from the sources into the basin would contribute to the inverse gradient. The constance of the quartz flux may be attributed to the mixing of fine quartz particles transported by the Antarctic bottom water, by ice rafting or by wind.

Bulk Sediment Geochemical Changes

We also analyzed the bulk geochemical composition of the carbonate-free fraction by instrumental neutron activation for 18 samples of core RC11-120 (Table 2). The lithogenic signal could be altered by hydrogenous-hydrothermal signal in case

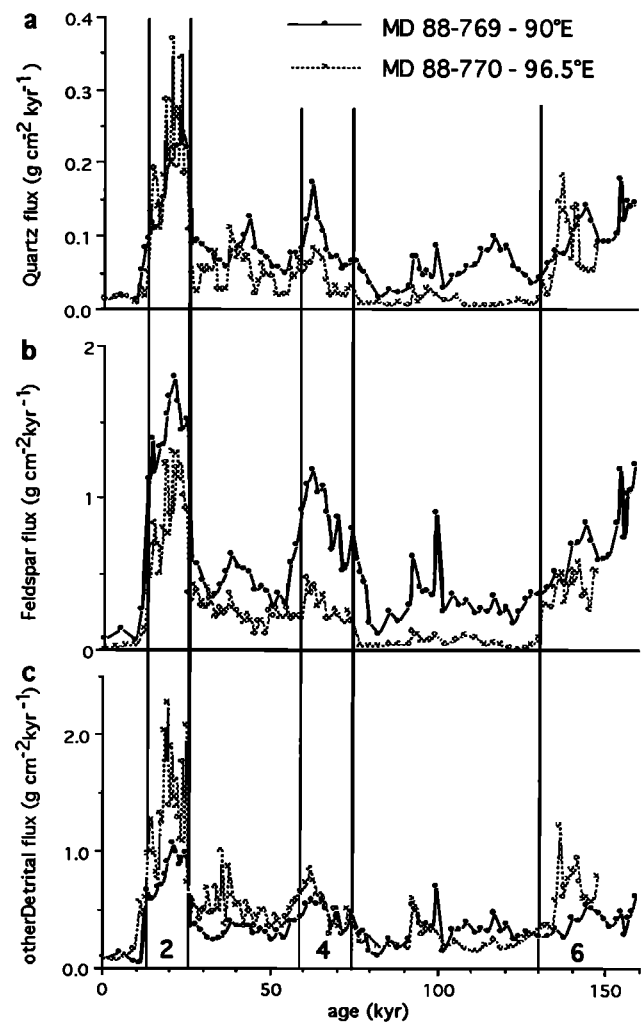


Figure 6. (a) Quartz flux changes, (b) Feldspar flux changes and (c) "other detrital" flux changes in the two cores MD 88-770 ($46^{\circ}01'S-96^{\circ}27'E$) and MD 88-769 ($46^{\circ}04'S-90^{\circ}06'E$) from the southeast Indian Ridge during the last climatic cycle. Glacial isotopic stages boundaries are represented by vertical line. All the flux are expressed in $\text{g cm}^{-2} \text{kyr}^{-1}$.

of coating by oxide or hydroxide of the grains analyzed. However, rare earth element analysis of the samples revealed no significant cerium anomaly, the latter being expected in case of hydrothermal component, ferromanganese nodules [Elderfield *et al.*, 1981; Ruhlin and Owen, 1985] or diagenetic products associated with an authigenic Fe-Mn-rich phase adsorbed onto the surface of particles [Elderfield *et al.*, 1981; Palmer, 1985]. In addition, there is no significant correlation between REE and Fe concentrations, diminishing the possibility of high Fe-Mn-rich contribution [Elderfield *et al.*, 1981; Palmer, 1985]. Consequently, we assume that geochemical composition of the carbonate-free fraction of this core represents more likely a lithogenic signal. These samples were selected in both major MS peaks and background over the last 180 kyr. Geochemical composition of the detrital material reveals very weak glacial-interglacial changes. However, the coldest events (isotopic stages 2, 4, and 6) are characterized by a very small increase in concentration of some trace elements (Fe, Ni, Sc, and Ta) which characterize primarily a mantle-derived origin [Grousset *et al.*, 1983; Grousset and Chesselet, 1986]. The example of iron is given in Figure 7. Similarly, although the variations are very weak, La/Ta and La/Sm ratios (Figure 7) slowly decrease during glacial periods indicating a likely volcanic contribution [Grousset *et al.*, 1982].

Sr Isotopic Composition of the Coarse Fraction

To identify further the origin and distribution of coarse glacial detrital inputs, we analysed the Sr isotopic composition of the >45 μm , carbonate-free fraction of samples corresponding to isotopic stage 2 in each core (Table 1) and of a beach sample from Kerguelen Island. Because of very small amount of >45- μm detrital material, we sampled large sediment volumes in the intervals corresponding to the isotopic stage 2. Although the Sr isotopic ratio of the >45- μm fraction might be slightly lower than the ratio obtained on the bulk sample [Dasch, 1969; Biscaye and Dasch, 1971], we

chose this approach because it is difficult to separate the fine detrital fraction from the opal fraction (small diatoms) without an alkaline dissolution which can remove not only opal but also some clay minerals. In consequence, the >45- μm size fraction could be biased towards particules transported by hydrographic processes such as sea-ice and iceberg transport and against both the fine (<7 μm) aeolian dusts found in Antarctic ice cores [Petit *et al.*, 1981, 1990; Mounier, 1988; Gaudichet *et al.*, 1986] and the fine fraction carried by bottom currents. In addition, because minerals from the same source probably come in different sizes, results on the >45- μm size fraction which neglect clays have to be interpreted carefully. After extracting the >45- μm detrital fraction from the opal fraction by several decantations and by picking out the remaining radiolaria, the samples were dissolved in PTFE beakers with 2b(HF+HClO₄+HNO₃) mixture and were chemically separated and analyzed by mass spectrometry following techniques previously described [Grousset *et al.*, 1988, 1990]. ⁸⁷Sr/⁸⁶Sr isotopic values are plotted against 1000/Sr ratios (Figure 8a). On such a plot, mixing lines linking end-members are always straight lines [Faure *et al.*, 1967].

Sr isotopic composition of the >45- μm detrital fraction from glacial samples (Table 1 and Figure 8a) includes data previously published concerning the Antarctic continent [De Paolo *et al.*, 1982; Grousset *et al.*, 1992], some volcanic Islands [O'Nions and Pankhurst, 1974; Hawkesworth *et al.*, 1977; Dosso *et al.*, 1979], the southeast Indian ridge rocks [Dosso *et al.*, 1988] and the potential dust and loess sources [Grousset *et al.*, 1992]. On the west-east transect we focused on the glacial detrital signatures are characterized by a mixture of two detrital end-members: the old Antarctic continental craton with high ⁸⁷Sr/⁸⁶Sr isotopic ratios (0.7134 to 0.7606) and the young volcanic Islands (Crozet, Kerguelen) with low ⁸⁷Sr/⁸⁶Sr isotopic ratios (0.70411 to 0.70765), similar to ratios of typical oceanic island basalt [Zindler *et al.*, 1981]. ⁸⁷Sr/⁸⁶Sr isotopic ratios are plotted against 1000/Sr (Figure 8a). They confirm an eastward decrease of the volcanic input contribution. In the western part of the basin the ⁸⁷Sr/⁸⁶Sr

Table 2. Geochemical Composition of the Carbonate-Free Fraction for 18 Samples of Core RC 11-120

Depth, cm	Age, kyr	Fe ₂ O ₃ , ppm	Ni, ppm	Sc, ppm	Ta, ppm	La, ppm	Ce, ppm	Sm, ppm	Eu, ppm	Tb, ppm	Yb, ppm	La/Ta	La/Sm
25	7.40	5.06	14	14.1	3.058	24.08	44.8	3.47	0.54	0.445	1.4	7.87	6.93
75	18.52	8.31	34	18.9	1.937	9.8	18.1	1.8	0.72	0.262	1.08	5.05	5.44
86	20.99	7.48	32	19.5	2.112	11.01	23	1.96	0.86	0.289	1.17	5.21	5.61
186	48.12	4.76	15	12.4	2.594	20.69	20.1	2.9	0.54	0.359	1.32	7.97	7.13
192	50.42	5.88	18	14.8	1.979	10.01	19.8	1.63	0.54	0.225	0.97	5.05	6.14
222	64.27	6.61	19	15.7	2.145	9.24	36.3	1.71	0.63	0.247	1.05	4.30	5.40
266	76.71	4.65	17	13.7	1.836	10.08	17.8	1.57	0.51	0.219	0.85	5.49	6.42
269	77.47	5.77	26	14.3	1.873	11.09	16.1	1.68	0.4	0.218	0.97	5.92	6.60
318	92.04	5.23	19	14.6	2.077	10.57	17.3	1.65	0.57	0.234	1.03	5.08	6.40
344	97.72	3.98	19	11.3	1.898	12.51	22	1.8	0.48	0.23	0.96	6.59	6.95
383	108.53	6.6	28	15.3	1.885	10.52	22.8	1.64	0.62	0.23	0.97	5.58	6.41
417	122.47	6.18	25	15.1	1.874	10.47	22.6	1.62	0.52	0.223	0.97	5.58	6.46
455	132.7	7.3	22	14.4	2.202	8.45	22.2	1.44	0.59	0.206	0.86	3.83	5.86
498	142.66	6.56	24	16.9	2.352	10.97	20.9	1.87	0.78	0.26	1.17	4.66	5.86
568	159.43	7.2	23	16	2.177	10.95	17.1	1.73	0.55	0.273	1.05	5.02	6.32
579	164.64	6.48	24	15.9	1.967	10.85	18.4	1.8	0.72	0.237	0.97	5.51	6.02
685	216.3	5.55	16	12.1	1.863	8.83	15.6	1.42	0.42	0.193	0.8	4.73	6.21
697	219.7	7.61	22	15.8	2.61	12.35	26.3	2.02	0.74	0.295	1.16	4.73	6.11

RC 11-120 (43°21' S - 79°52' E)

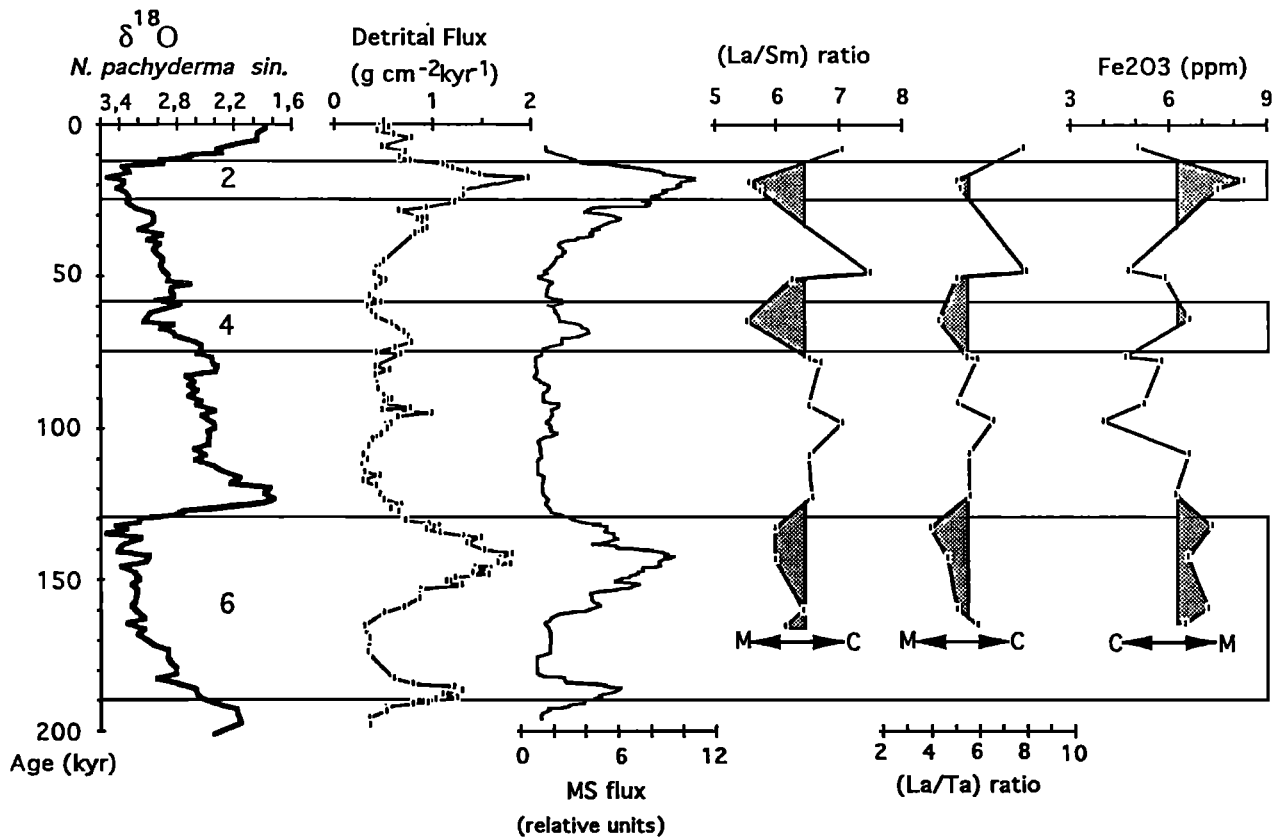


Figure 7. Downcore evolution of $\delta^{18}\text{O}$ measured on *N. pachyderma sin.*, detrital flux, MS flux, La/Sm ratio, La/Ta ratio and Fe_2O_3 content (ppm) in the core RC11-120 during the past 200,000 years. Glacial isotopic stages are represented by shaded bands.

signature is typically volcanic (0.7042 to 0.7069), whereas a typical Antarctic signature is observed in the core collected near the Antarctic continent (0.7317). In the eastern part of the basin, the $^{87}\text{Sr}/^{86}\text{Sr}$ signature characterizes a mixing between the two main sources (0.7124). From the $^{87}\text{Sr}/^{86}\text{Sr}$ isotopic ratio versus $1000/\text{Sr}$ diagram (Figure 8a) we may exclude South Sandwich Island (SSI), southeast Indian Ridge, Australian and South American dusts, as main potential sources for this material. Considering that we had a two end-member mixing model (Figure 8a), we estimated the volcanic contribution in all the glacial samples, especially along the eastward decreasing gradient in lithogenic fluxes. Because of the large range of Sr isotopic ratios and concentrations observed in the Antarctic source, we selected three potential Antarctic compositions: a/ $[\text{Sr}]=68$ ppm and $^{87}\text{Sr}/^{86}\text{Sr}=0.76$, b/ $[\text{Sr}]=104$ ppm and $^{87}\text{Sr}/^{86}\text{Sr}=0.74$, and c/ $[\text{Sr}]=200$ ppm and $^{87}\text{Sr}/^{86}\text{Sr}=0.72$. Using $[\text{Sr}]=1000$ ppm and $^{87}\text{Sr}/^{86}\text{Sr}=0.705$ for the Kerguelen-Crozet derived particles, we estimated a volcanic contribution of about 60-70% close to the Kerguelen and Crozet Plateaus, decreasing to only 10% in the eastern part of the basin (Figure 8b). When we apply the three different values selected for the Antarctic end-member we obtain similar contributions at $\pm 10\%$. These results indicate that the volcanic province of Kerguelen-Crozet contributes for

more than half of the coarse particle ($>45\ \mu\text{m}$) flux as far as $90\text{--}110^\circ\text{E}$. Eastward the Antarctic becomes the major source of coarse lithogenic particles.

Discussion: Sediment Supply and Transport Mechanisms

The movement of Antarctic Bottom Water (AABW), which forms along the Adélie Land coast and in the Ross Sea [Jacobs *et al.*, 1970; Eittrheim *et al.*, 1972 a, b], is generally clockwise in the southeast Indian basin. AABW, which travels westward close to the Antarctic continent, is diverted to the north by the Kerguelen Plateau, and then it flows to the east along the southeast Indian Ridge [Kennett and Watkins, 1975, 1976; Kolla *et al.*, 1976]. The influence of the northward moving AABW on sediment transport and deposition was previously demonstrated [Kolla and Biscaye, 1976; Kolla *et al.*, 1978]. Kolla *et al.* [1978] indicated a clear relationship between dispersal of quartz and clay minerals and AABW movement, using both bottom water turbidity measurements and mineralogy of sediments. As a first approximation, modern terrigenous dispersal, as recorded by both detrital and MS flux distribution, confirms that sediment distribution is mainly influenced by AABW, as previously assumed by Kolla *et al.*

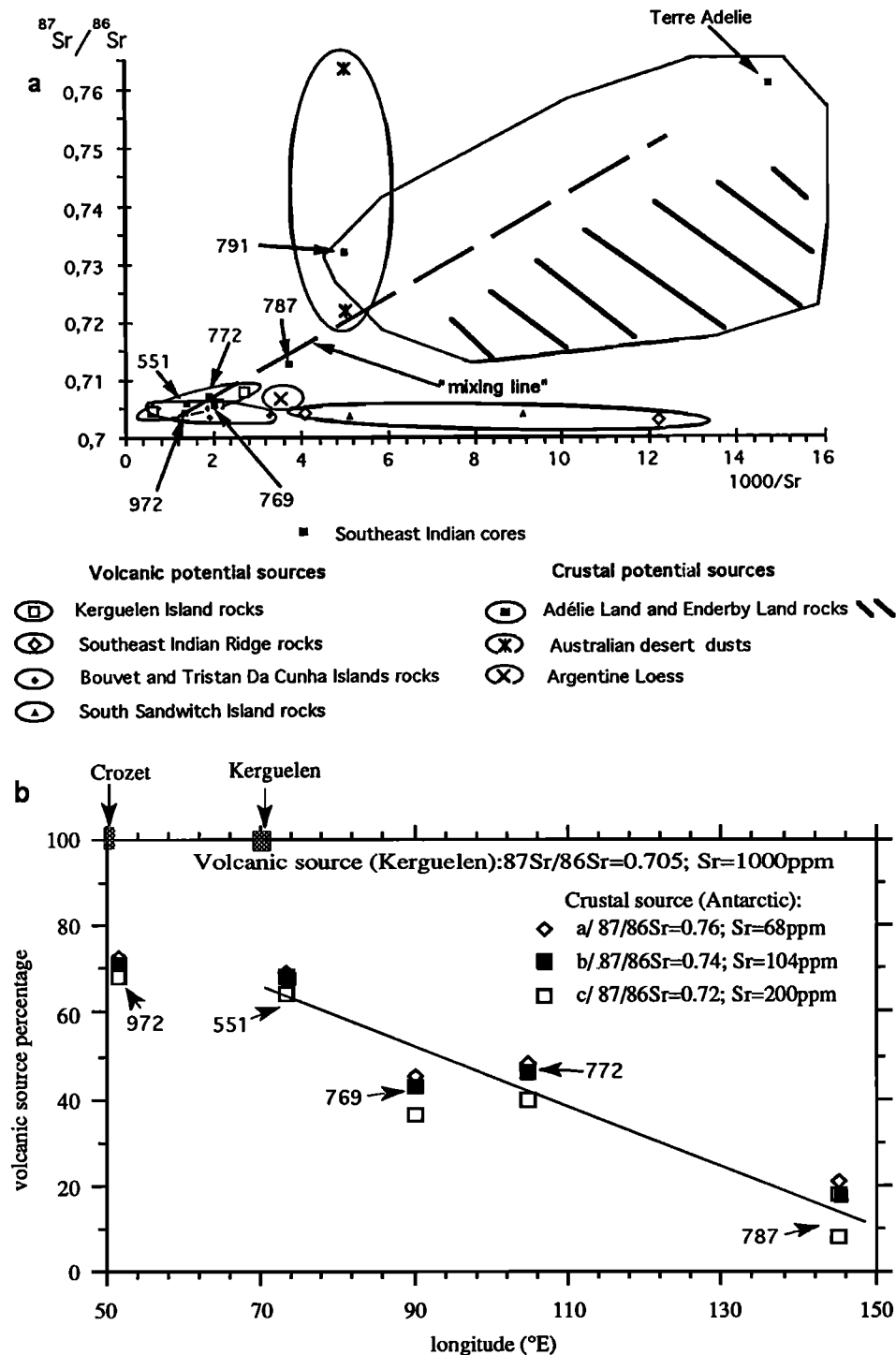


Figure 8. (a) The $^{87}\text{Sr}/^{86}\text{Sr}$ isotopic ratio versus $1000/\text{Sr}$ plot for the $>45\text{-}\mu\text{m}$ detrital fraction from glacial samples (isotopic stage 2) for the southeast Indian basin and for the potential detrital sources from the southeast Indian and Atlantic sectors of the southern ocean (data are given in the Table 1), (b) distribution of the calculated volcanic source contribution (in percent) to the $>45\text{-}\mu\text{m}$ detrital fraction along a transect from Kerguelen to Tasmania.

[1978]. However, the Kerguelen volcanogenic contribution that we clearly observe along the southern flank of the southeast Indian ridge, suggests a direct input of material from the Kerguelen Plateau. Kolla and Biscaye [1976] and Kolla *et al.* [1978] did not take into account that the Circumpolar Deep

Water (CDW) transport direction is the same as that of the AABW. Then, the west-to-east particles transport can be associated either with AABW or CDW movements. The circulation of the AABW is linked to the displacement of a nepheloid layer which incorporates terrigenous particles from

both dense shelf water and bottom sediments [Barron *et al.*, 1989; Ehrmann and Grobe, 1991]. AABW particle load mostly settles along the western margin of the basin [Ettreim *et al.*, 1972a] building a large sedimentary ridge parallel to the eastern flank of the Kerguelen Plateau [Houtz *et al.*, 1977]. As a result, only minor amounts of particles reach the southern flank of the southeast Indian Ridge, as suggested by low bottom-water turbidity [Ettreim *et al.*, 1972a; Kolla *et al.*, 1978]. Suspended particles could be added to the nepheloid layer found along the southern flank of the southeast Indian ridge by interaction of moving water (ACC-CDW) with the top and western slope of the Kerguelen Plateau. This assumption is supported by the high proportion of smectite from volcanic origin found along the southeast Indian Ridge. Present-day wind stress produces an ACC that occurs from 45°S to 50°S [Klinck and Smith, 1993]. This region includes the northern part of the Kerguelen Plateau. Hydrographic profiles from the southern Indian Ocean [Gordon and Molinelli, 1975] show that the AABW is observed at depths greater than 3500 m on the southern flank of the southeast Indian Ridge. Using recent deep-sea benthic foraminifers, Corliss [1979] found that AABW influences the eastern sector, the top and north flank of the southeast Indian Ridge, whereas the western southeast Indian Ridge is rather associated with CDW. In addition, AABW mixes with circumpolar deep water as it moves from the Antarctic continental shelf to the southern flank of the southeast Indian Ridge. The five cores from the southeast Indian ridge were collected from waters between 3000 and 3500 m. Consequently, we cannot exclusively attribute the detrital distribution to the AABW, but we suggest that sediment transport on the bottom is associated with a mixture of AABW and CDW influence.

Because most of our cores are located along the southern flank of the southeast Indian ridge, that is, in the west-to-east decreasing gradient in detrital flux from Kerguelen, we will focus on this transect in the following discussion. In addition, this area is probably the most sensitive place to record AABW, ACC-CDW and ice-rafting transports. High detrital fluxes are observed during glacial periods. Are they a reflection of changes in ice-rafting discharges, as observed in the northern hemisphere during the same period [Grousset *et al.*, 1993]? Are they induced by an aeolian contribution or simply by changes in bottom water current velocity? The glacial terrigenous material consists mainly of fine-grained particles with small amount of coarse particles. This suggests that the main transport/deposition mechanism should probably be attributed to relative contribution of advection by intermediate water masses or benthic nepheloid layer, to aeolian input, and to ice rafting transport.

Antarctic Ice-Rafted Detritus Input

Cooke [1978] and Cooke and Hays [1982] indicated very low coarse ice-rafting contribution ($>150\text{-}\mu\text{m}$ ice-rafted detritus fluxes lower than $20\text{ mg cm}^{-2}\text{ kyr}^{-1}$) in the southeast Indian Ocean during glacial times. On the basis of the glacial detrital flux recorded in the southeast Indian Ocean (from $3\text{ g cm}^{-2}\text{ kyr}^{-1}$ in the western part of the basin where the fluxes are maximum to $1\text{ g cm}^{-2}\text{ kyr}^{-1}$ in the eastern part), and even though the $>150\text{-}\mu\text{m}$ fraction represents only one tenth of the

total ice-rafted detritus (IRD) flux, we suggest that IRD represented probably less than 20% of the total detrital input. Therefore we exclude ice rafting as the main transport mechanism of detrital material during the glacial periods. Nevertheless, we analyzed this fraction because ice-rafted particles can yield some information about changes in surface water hydrography and ice sheet dynamics, in relation with climatic changes. Isotopic results on the coarse fraction suggest a mixing of ice-rafted particles originated from volcanic source, probably coming from the Kerguelen and Crozet archipelago and an Antarctic source. We suppose that most of the coarse detrital material originating from Antarctica was transported to the Southeast Indian sector mainly by icebergs from the eastern Antarctic (from the Ross Sea to Enderby Land) along with a variable amount of icebergs from the western Antarctic. Icebergs probably traveled away from the continental margin via the Antarctic Circumpolar current as observed today in the south Indian Ocean [Jacobs, 1992]. We cannot rule out the possibility that some of the volcanic components could originate from the Antarctic Peninsula because strontium isotopic characteristics of this potential source are not known. Indeed, evidence of western Antarctic Peninsula contribution in coarse detrital particles to the southeast Indian sector was recently demonstrated (M. Paterné *et al.*, Massive iceberg discharge of the western Antarctic ice-sheet during the last glacial, submitted to *Nature*, 1994). Seven levels of glass shards originating from the western Antarctic Peninsula were recognized by these authors in the glacial section of two cores (MD 88-769 and MD 88-770). Furthermore, dispersed ashes of calc-alkaline composition were found in Quaternary series of the southwest part of the southeast Indian basin, suggesting a probable South Sandwich Island (SSI) origin for some volcanic particles [Morche *et al.*, 1991]. In addition, because we have not studied glacial-interglacial transition with a high enough resolution, we cannot dismiss the possibility of important glacial Atlantic input during at least some short episodes. A study on a high-resolution mode still has to be carried out in order to recognize and separate minor ice-rafting contribution. IRD derived from the Kerguelen province, reflect either the presence of an ice sheet on the Kerguelen Island or seasonal sea-ice cover. Consequently, although our results demonstrate a reduce ice rafting contribution in the southeast Indian basin, low sea level stands during glacial times could have induced ice sheets instability resulting in larger input of icebergs to the southern ocean.

Aeolian Input

Variability of quartz flux recorded in cores from the southeast Indian Ridge (Figure 6) is in good agreement with previous investigations on Southern Hemisphere marine sediments [Kolla and Biscaye, 1976; Thiede, 1979]. During glacial periods, high quartz content recorded in sediments and in New Zealand loess [Alloway *et al.*, 1992] have been linked to extension of arid source areas and to enhancement of atmospheric circulation [Petit *et al.*, 1990]. Glacial high particule fluxes were also observed in Antarctic ice cores [Petit *et al.*, 1981, 1990; De Angelis *et al.*, 1987]: these particle can only be aeolian in origin. In oceanic sediments, however, the

clay fraction accumulated onto the southeast Indian Ridge commonly consists of smectites [Griffin *et al.*, 1968; Kolla and Biscaye, 1976; this work] and very small amount (less than 10%) of typical airborne clay minerals from desert source areas [Griffin *et al.*, 1968]. These typical airborne clay minerals are found in Antarctic ice cores [De Angelis *et al.*, 1987; Gaudichet *et al.*, 1986, 1988]. In addition, assuming that aeolian particles contain about 13% of quartz [Gaudichet *et al.*, 1986], an eolian flux 600 times higher than the one recorded in the Antarctic ice sheet would be required to explain the quartz flux observed in this area during glacial times. A dust flux comparable to the one recorded in the east Antarctic ice sheet ($2 \text{ mg cm}^{-2} \text{ kyr}^{-1}$) (L. H. Burckle *et al.*, Correlation between Vostok dust and *E. antarctica* (diatom) relative abundance records in high southern latitudes, submitted to *Nature*, 1994) (hereinafter referred to as Burckle *et al.*, 1994) would represent less than 1% of the total detrital flux measure in the southeast Indian basin. Furthermore, Duce *et al.* [1991] showed modern aeolian fluxes of 0.001 to $0.01 \text{ g cm}^{-2} \text{ kyr}^{-1}$ for the southern ocean. Assuming that Vostok dust flux were greater by a factor 15 during the last glacial maximum [Petit *et al.*, 1990], glacial dust flux to the southern ocean would be about 0.15 to $0.015 \text{ g cm}^{-2} \text{ kyr}^{-1}$, representing less than 5% of the total detrital flux of the southeast Indian sector. Consequently, hydrographic transport is the likely explanation for detrital flux in this basin and we believe that the aeolian signal is just too small to be detected and cannot be considered a major component of marine sediments from the southeast Indian Ocean.

Deepwater Circulation (AABW and ACC-CDW)

Mineralogical, geochemical, and isotopic results suggest that no major change occurred in the accumulation patterns from the southeast Indian basin during glacial periods. Enhancement of volcanic material input composed of fine minerals (felspars, smectites, volcanic glasses and ashes) and enriched in Fe, Ni, Sc, Ta (Table 2), mixed with quartz and other minerals of probable continental origin (mainly the Antarctic craton), supports the idea of a main transport in suspension by deepwater currents along both Antarctica and the Kerguelen plateau. During coldest periods, an eastward flux gradient occurred, but fluxes were higher than today. A more important contribution of the sources is thus required to explain the higher glacial detrital fluxes. During periods of glaciation, as a result of lower sea level stands, larger continental shelf surfaces were exposed and available for erosion. Moreover, a small ice cap covered Kerguelen Island. Larger amount of terrigenous particles and volcanic products could be eroded, reworked, and transported from the shelves and shallow plateaus to the deep basins. Compared to interglacial periods where most of the detrital particles were trapped onto the shelves, transportation to the deep-sea through the action of bottom currents, turbidity currents or slumping should have been more efficient during glacials. During transport, most of the fine material reached the deep basin, whereas the coarse fraction probably accumulated on the continental slope or in the deep-basin along the margins. The fine fraction could be integrated in the bottom water circulation and then dispersed away by a nepheloid layer,

which could have been denser during glacial periods compared to interglacials because of a stronger input of fine particles to the deep-sea. Clay mineralogy from the Southernmost areas of the southern ocean reveals high amounts of illite-chlorite [Hampton *et al.*, 1987; Ehrmann *et al.*, 1992]. On the other hand, an important stock of smectite is available on the Kerguelen plateau both from old and recent sediments [Chapuy, 1988; Ehrmann *et al.*, 1992]. Thus the removal and transport of smectite-rich clays from southern ocean volcanic regions (the Crozet Plateau-Island and Kerguelen Plateau regions) would better explain the high smectite content found on the southeast Indian Ridge during glacial periods. In addition, the rapid decrease in feldspar flux to the East combined to a important flux of clay could confirm a differential transport based on size and density of particles. The dense and large size particles like feldspar, pyroxene, etc, settled down quickly, whereas the fine particles (mainly smectite) were transported far away probably both by the ACC and by bottom water (AABW). Clay mineral assemblages from the southwest part of the basin show a higher proportion of illite and chlorite, which are characteristic of physically weathered rocks from the East Antarctic craton [Ehrmann and Grobe, 1991]. This observation suggests that the Kerguelen source contribution decreases to the south. Antarctic fine particles from the shelf and the continental slope are the major source in the southern part of the basin. In fact, we have probably a variable mixture of the two components, depending on the distance from their source.

A possible enhancement of water mass circulation combined with the weaker stability of shelves and shallow plateaus could also have contributed to a stronger transfer of terrigenous products. However, there is no clear evidence of higher AABW velocity during glacials. Recent results obtained in the Weddell Sea even suggest that during the coldest periods, when sea ice cover was more extensive than today, bottom currents were weaker [Pudsey, 1992]. A same conclusion has been made for the North Atlantic Deep Water [Duplessy *et al.*, 1988]. Ehrmann and Grobe [1991] found cyclic changes in Pleistocene sedimentation from the southwest part of the southeast Indian basin (sites 745 and 746, ODP leg 119). Sedimentological characteristics from the cyclic facies were related to glacial and interglacial cycles. This would indicate that the AABW circulation was less erosive in the southeast Indian basin during glacial periods than during interglacial times [Ehrmann and Grobe, 1991]. AABW formation is related to two mechanisms: (1) deep convection in the open ocean triggered by increasing salinity in surface waters during sea ice formation [Gordon, 1978, 1982; Killworth, 1979; Gordon and Huber, 1984] and (2) mixing processes mainly off ice shelves and on continental slopes [Foster and Middleton, 1979; Foldvik *et al.*, 1985; Foster *et al.*, 1987]. During glacial times, the grounding lines of ice shelves moved seaward and stopped at or close to the shelf break. As a result, larger parts of ice shelves were linked to the sea bed and flow of water beneath the ice was reduced, forming less cold, dense ice shelf water (ISW). Decrease in ISW formation and in flow of NADW to the southern ocean [Duplessy *et al.*, 1988], which are the two water masses mixing together to form new AABW, would induce a decreasing AABW formation. Greater permanent sea ice

coverage during the same period would also result in a reduction of AABW formation. Consequently, we cannot invoke a more erosive AABW circulation to explain higher glacial detrital flux. Another possibility could be the enhancement of the ACC-CDW. Because of its close relation to wind stress [Nowlin and Klinck, 1986], the ACC could have changed both in strength and in position in response to wind stress change. Using a simple wind-driven model, Klinck and Smith [1993] indicated that a wind strength enhancement over the southern ocean would result in increased transport by the ACC during glacial times. Unfortunately, although this model is in agreement with an increased thermal gradient (as recorded in deep-sea sediments), it fails to simulate a latitudinal displacement of the ACC. Although evidence of ACC strength changes are still missing for late Quaternary, we cannot ignore that a possible increased in the ACC could have contribute to higher deep-sea detrital fluxes during cold periods.

Comparison to Vostok Dust Flux Record

Our data do not suggest that MS records any aeolian input. Consequently, the stratigraphic approach proposed by Petit *et al.* [1990] for the Vostok dust ice core content, which was based upon the assumption that MS record in the marine deep-sea core RC11-120 reflected aeolian input, must be discussed. Their interpretation did not exclude that ice (Vostok) and marine records were approximately in phase during the last glacial/interglacial cycle. Recently, Pichon *et al.* [1992] indicated broad similarities between the summer sea-surface temperature (SST) changes of southern waters at 55°S and air temperature over Antarctica at Vostok. Because strong

climatic connections should exist between the Antarctic and surrounding waters, SST changes in high latitudes influence the temperature over Antarctica by transfer of heat and atmospheric water, these authors proposed timescales to fit both temperature records. The Vostok record adjustments made by Pichon *et al.* [1992] are in agreement with those suggested by Petit *et al.* [1990]. Using this new chronostratigraphy, we recalculated the Vostok dust flux (Vostok dust concentration multiplied by ice deposition rate and by a mean dust density of about 2.65 g cm⁻³). As previously indicated by Petit *et al.* [1990], three peaks of higher dust flux (Figure 2b in the work by Petit *et al.* [1990] and Figure 9a) are recognized for the Vostok record during the past 150 kyr corresponding to glacial marine isotopic stages 2, 4, and 6. Comparison of detrital flux records from marine cores of the southeast Indian Ocean with recalculated Vostok dust flux reveals a remarkable agreement among the records (Figure 9). These similarities suggest that both changes in atmospheric dust input and changes in detrital input to the deep basins are linked to the same global phenomenon: global climate dynamics (global ice volume). In fact, detrital flux increase observed in the Southern Ocean might be the result of (1) low sea level stands, which induce shelves and shallow plateaus destabilisation and ice sheets unstability (resulting in increasing input of icebergs) and (2) to a lesser extent of an increase in oceanic circulation (ACC). Vostok dust deposition has been interpreted as depending on periods of aridity, wind speed over source areas and meridional transport efficiency [Petit *et al.*, 1990]. However, Clemens and Prell [1990] and Rea [1990] related dust flux to dust source-area aridity but not to wind strength. In the following discussion, we prefer to interpret dust input in term of changes in dust source rather than change in atmospheric circulation. Low sea level stands induced an increase in the exposure of major continental shelves, resulting

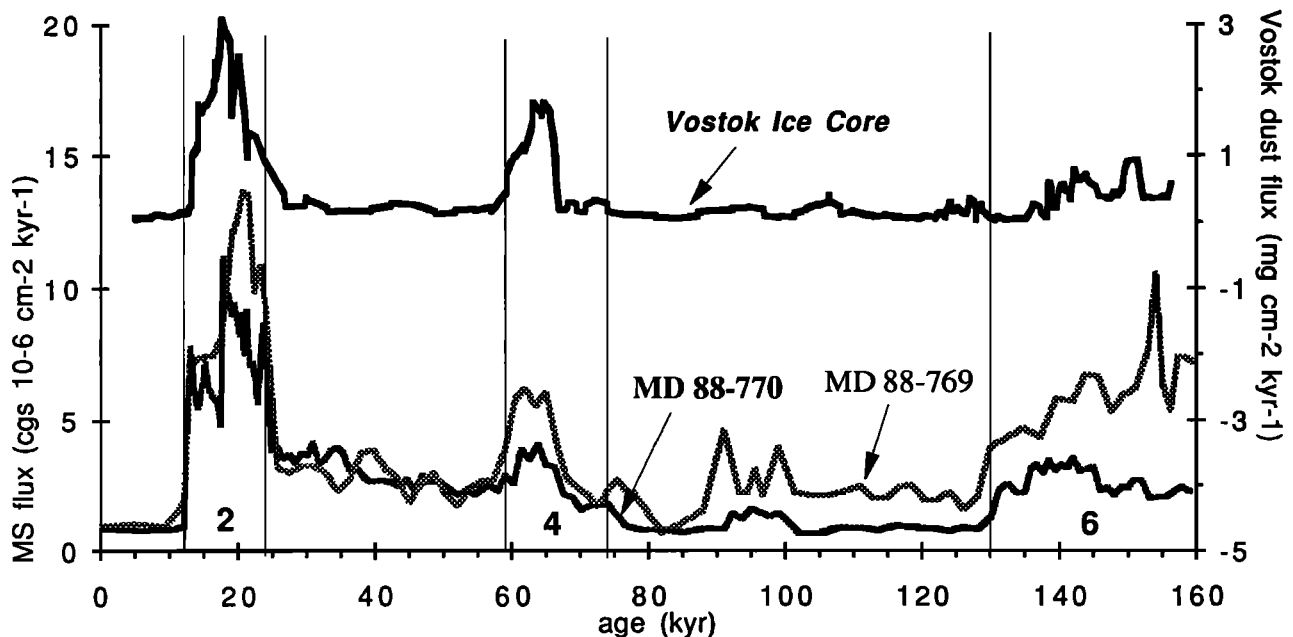


Figure 9. Comparison of MS flux of the cores MD 88-769 and MD 88-770 to Antarctic ice core dust accumulation rate recalculate using Pichon *et al.* [1992] chronostratigraphy for Vostok ice core for the past 150,000 years. Glacial isotopic stages boundaries are represented by vertical lines.

in higher mass of dust particles available for aeolian transport. If continental shelves played an important role in providing terrigenous particles both to the atmosphere and to the oceans, changes in exposed continental shelf surface could be a critical parameter modulating the intensity of particle flux. Burckle et al. (1994) calculated that during Melt Water Pulse 1A in the northern hemisphere [Fairbanks, 1989; Charles and Fairbanks, 1992], about 65% of the exposed Argentine continental shelf was submerged by rising sea level. Because the overwhelming majority of last glacial maximum dust from East Antarctica are of Argentine continental shelf origin [Grousset et al., 1992], dust input to Antarctica should have been drastically reduced during this episode. Vostok dust flux curve shows a sharp decrease of dust input (Figure 9a) during the Melt Water Pulse 1A about 12.2 to 12.6 kyr B.P. [Fairbanks, 1989]. During the same time the major continental shelves and shallow plateaus including the Kerguelen-Crozet Plateau became more stable, thus reducing the input of fine detrital particles to the deep basin of the southeast Indian Ocean. Indeed, detrital inputs strongly decrease in the southeast Indian basin at this time (Figure 9b). Consequently, we suggest that changes in southern ocean terrigenous flux coeval with changes in dust accumulation on Antarctica because both respond to internal climate-related forcing mechanisms (e.g., global ice volume).

Summary and Conclusions

Considering the evolution of detrital particle accumulations in the Southeast Indian Ocean, we identified three periods of high detrital input during the last climatic cycle, corresponding to marine glacial isotopic stages 2, 4, and 6. Mineralogical, geochemical and Sr isotopic composition of glacial detrital inputs indicate that these events result mostly

from both mantle-derived (volcanic) inputs (Kerguelen and Crozet Plateaus and Islands) and crustal origin (mainly the Antarctic continent). These detrital peaks characterizing glacial periods appear to be mainly due to hydrographic rather than aeolian transport. Similar detrital flux distributions, west-to-east gradients, characterize both glacial and interglacial periods, with a strong enhancement during glacial stages. The Sr isotopic composition of the glacial detrital fraction $>45 \mu\text{m}$ suggests that this eastward gradient reflects the eastward transport of volcanic material originating from the Kerguelen province which mixes with Antarctic-derived material; both are brought mainly by ACC-CDW/AABW and to a lesser extent by ice rafting. High detrital inputs during glacial times suggest a more efficient transfer of both volcanic and crustal detrital material to the Southeast Indian basin which could be interpreted as a result of (1) more important continental exposure due to lowered sea level, (2) of ice sheets instability resulting in larger input of icebergs than today, and (3) perhaps to a lesser extent of an enhancement of ACC.

We observe a good visual correlation between detrital flux records in the southeast Indian Ocean and Vostok ice core dust record. This suggests a common global control on both aeolian and marine detrital inputs: global ice volume. Other studies on a high-resolution basis are needed to confirm these results.

Appendix A

See Table A1, which shows an example of core data (Detrital, Magnetic Susceptibility, and Mineralogical data) downloaded into the NGDC database.

Table A1. Detrital, Magnetic Susceptibility, and Mineralogical Data for Deep-Sea Core MD 88-769 (46° 04' S - 90° 06' E)

Depth, cm	Age, kyr	DBD, g cm ⁻³	SR, cm kyr ⁻¹	Detrital, wt%	Quartz, wt%	MS cm ³ , c.g.s. 10 ⁻⁶	MS, flux	Detrital, flux	Quartz, flux	Feldspar, flux	Other Detr., flux
0	4.61	0.63	9	14.89	1.2	0.29	2.63	0.30	0.015	0.09	0.09
10	6.46	0.76	9	19.34	1.4	0.32	2.86	0.49	0.022	0.15	0.15
20	8.30	0.76	9	9.08	0.9	0.29	2.63	0.23	0.015	0.07	0.06
30	10.15	0.69	9	13.08	1.1	0.42	3.74	0.3	0.056	0.28	0.06
50	13.1	0.47	9.1	45.03	2.3	0.77	7.0	1.91	0.099	1.13	0.68
60	14.2	0.41	9.1	56.37	3.2	0.81	7.32	2.12	0.12	1.4	0.60
65	14.75	0.39	9.1	53.94	3.2			1.9	0.112	1.18	0.60
70	15.3	0.39	9.1	59.29		0.82	7.43	2.08			
80	16.4	0.41	9.1	58.67	3.8	0.82	7.43	2.20	0.14	1.35	0.71
90	17.5	0.41	9.1	59.66	4.1	0.89	8.09	2.24	0.153	1.36	0.73
100	18.31	0.37	12.3	55.99	4.2	0.81	9.91	2.57	0.192	1.56	0.82
110	19.13	0.37	12.3	61.26	4.5	1.0	12.03	2.81	0.204	1.68	0.93
130	20.75	0.4	12.3	63.2	4.5	1.11	13.66	3.11	0.222	1.81	1.08
140	21.56	0.4	12.3	58.44	4.6	1.10	13.51	2.88	0.224	1.64	1.0
150	22.38	0.4	12.3	52.43	4.7	0.81	9.91	2.58	0.233	1.45	0.9
160	23.19	0.4	12.3	53.91	4.9	0.88	10.83	2.65	0.244	1.46	0.95
170	24.0	0.37	12.3	60.13	4.8	0.77	9.48	2.76	0.222	1.53	1.01
180	25.75	0.36	5.7	51.87	4.5	0.56	3.21	1.08	0.092	0.60	0.38
190	27.5	0.36	5.7	51.75	4.6	0.53	3.0	1.06	0.096	0.58	0.39
200	29.25	0.32	5.7	49.24	4.8	0.57	3.27	0.9	0.089	0.47	0.34
210	31.0	0.32	5.7	38.22	4.5	0.57	3.27	0.7	0.082	0.36	0.26
220	32.75	0.32	5.7	38.68	3.8	0.53	3.0	0.71	0.070	0.38	0.26
230	34.5	0.36	5.7	37.74	3.3	0.40	2.3	0.78	0.068	0.44	0.27

Table A1. (continued)

Depth, cm	Age, kyr	DBD, g cm ⁻³	SR, cm kyr ⁻¹	Detrital, wt%	Quartz, wt%	MS cm ⁻³ , c.g.s. 10 ⁻⁶	MS, flux	Detrital, flux	Quartz, flux	Feldspar, flux	Other Detr., flux
240	36.25	0.43	5.7	36.7	2.5	0.49	2.79	0.89	0.061	0.52	0.31
250	38.0	0.43	5.7	46.61	3.3	0.66	3.77	1.14	0.082	0.64	0.41
260	39.75	0.41	5.7	43.04	3.7	0.67	3.84	1.02	0.088	0.56	0.37
270	41.5	0.39	5.7	46.55	4.7	0.55	3.14	1.03	0.104	0.55	0.38
280	43.25	0.39	5.7	46.24	5.8	0.49	2.79	1.02	0.128	0.53	0.37
290	45.0	0.41	5.7	33.87	3.6	0.33	1.89	0.8	0.085	0.40	0.31
300	46.75	0.48	5.7	31.33	2.8	0.45	2.59	0.86	0.078	0.43	0.35
310	48.5	0.43	5.7	32.51	3.0	0.53	3.0	0.79	0.072	0.39	0.33
320	50.25	0.44	5.7	24.28	2.3	0.39	2.23	0.61	0.059	0.30	0.25
330	52.0	0.47	5.7	28.94	2.2	0.31	1.74	0.77	0.060	0.38	0.33
340	53.75	0.49	5.7	22.8	1.8	0.42	2.37	0.64	0.051	0.32	0.27
350	55.5	0.6	5.7	31.65	2.3	0.47	2.66	1.09	0.078	0.59	0.42
360	57.25	0.53	5.7	39.64	2.6	0.48	2.71	1.21	0.079	0.71	0.42
370	59.0	0.64	5.7	40.17	2.3	0.67	3.84	1.47	0.086	0.93	0.46
380	60.5	0.55	6.7	49.02	3.4	0.87	5.78	1.79	0.125	1.10	0.56
390	62.0	0.55	6.7	54.05	4.8	0.93	6.18	1.97	0.175	1.2	0.6
400	63.5	0.52	6.7	49.95	3.6	0.83	5.53	1.73	0.126	1.05	0.56
410	65.0	0.52	6.7	52.18	3.2	0.90	6.02	1.81	0.11	1.09	0.60
420	66.5	0.52	6.7	43.86	2.4	0.62	4.15	1.52	0.083	0.92	0.52
430	68.0	0.48	6.7	34.98	2.3	0.42	2.77	1.12	0.072	0.67	0.37
440	69.5	0.55	6.7	40.83	2.0	0.37	2.43	1.49	0.074	0.89	0.52
450	71.0	0.47	6.7	29.06	1.9	0.33	2.2	0.90	0.058	0.54	0.31
460	72.5	0.53	6.7	27.12	1.8	0.26	1.72	0.96	0.062	0.57	0.33
470	74.0	0.63	6.7	32.86	1.7	0.34	2.28	1.37	0.069	0.81	0.49
480	75.25	0.61	8	21.32	1.4	0.34	2.74	1.05	0.068	0.61	0.36
490	76.5	0.55	8	20.37	1.3	0.29	2.34	0.89	0.057	0.52	0.31
500	77.75	0.69	8	15.41	1.0	0.28	2.24	0.85	0.054	0.46	0.34
510	79.0	0.69	8	7.15	0.7	0.22	1.76	0.4	0.039	0.20	0.16
520	82.0	0.8	3.3	9.77	0.7	0.21	0.69	0.26	0.02	0.12	0.12
530	85.0	0.77	3.3	21.75	1.2	0.33	1.1	0.56	0.031	0.26	0.27
540	88.0	0.68	3.3	17.94	1.1	0.47	1.55	0.41	0.026	0.20	0.18
550	91.0	0.52	8.7	34.83	2.0	0.53	4.59	1.58	0.034	0.31	0.26
560	92.14	0.6	8.7	23.99	1.4	0.40	3.52	1.26	0.074	0.63	0.56
570	93.28	0.6	8.7		1.4	0.26	2.25		0.074		
580	94.42	0.63	8.7	16.3	1.1	0.26	2.25	0.89	0.058	0.43	0.41
590	95.57	0.63	8.7	15.25	0.9	0.36	3.10	0.84	0.049	0.40	0.39
600	96.71	0.75	8.7	13.29	0.9	0.25	2.14	0.87	0.056	0.41	0.40
610	97.85	0.64	8.7	14.08	0.8	0.34	3.0	0.79	0.047	0.37	0.37
620	99.0	0.65	8.7	30.44	1.6	0.45	3.96	1.74	0.09	0.92	0.73
630	101.4	0.61	4.2	18.13	1.3	0.54	2.24	0.46	0.033	0.27	0.16
640	103.8	0.55	4.2	34.3	2.1	0.51	2.14	0.78	0.049	0.39	0.34
650	106.2	0.6	4.2	28.65	2.0	0.51	2.14	0.72	0.051	0.31	0.35
660	108.6	0.53	4.2	37.27	2.8	0.55	2.29	0.83	0.062	0.35	0.42
670	111.0	0.43	4.2	36.04	3.6	0.60	2.49	0.64	0.063	0.26	0.32
680	112.85	0.43	5.4	31.81	3.7	0.4	2.03	0.73	0.085	0.29	0.36
690	114.71	0.45	5.4	27.78	3.5	0.38	2.03	0.68	0.084	0.27	0.33
700	116.57	0.49	5.4	36.63	3.9	0.45	2.44	0.97	0.104	0.38	0.49
710	118.43	0.52	5.4	23.92	3.0	0.48	2.56	0.7	0.083	0.26	0.33
720	120.28	0.62	5.4	23.35	2.7	0.37	1.96	0.79	0.09	0.30	0.40
730	122.14	0.71	5.4	13.8	1.6	0.37	1.96	0.53	0.063	0.20	0.27
740	124.0	0.75	5.4	15.4	1.4	0.42	2.23	0.62	0.057	0.26	0.30
750	126.0	0.73	5	20.02	1.4	0.32	1.59	0.73	0.05	0.35	0.34
760	128.0	0.79	5	19.1	1.0	0.41	2.05	0.75	0.039	0.40	0.32
770	130.0	0.71	5	20.42	1.4	0.79	3.96	0.72	0.048	0.39	0.29
780	132.4	0.57	4.2	32.92	2.8	1.04	4.32	0.79	0.066	0.43	0.29
790	134.8	0.49	4.2	47.43	4.0	1.12	4.68	0.97	0.083	0.54	0.36
800	137.2	0.48	4.2	41.01	4.0	1.04	4.32	0.82	0.079	0.46	0.28
810	139.6	0.52	4.2	59.18	5.1	1.39	5.80	1.28	0.111	0.72	0.45
820	142.0	0.53	4.2	57.43	5.8	1.37	5.7	1.28	0.128	0.75	0.42
830	143.83	0.52	5.5	55.22	5.1	1.23	6.72	1.57	0.146	0.86	0.56
840	145.67	0.51	5.5	50.52	4.5	1.22	6.66	1.4	0.124	0.74	0.54
850	147.5	0.51	5.5	43.09	3.5	0.98	5.33	1.19	0.095	0.61	0.49
860	149.33	0.51	5.5	41.89	3.5	1.09	5.93	1.16	0.095	0.63	0.44
870	151.17	0.45	5.5	45.2	3.9	1.14	6.19	1.12	0.096	0.64	0.38
880	153.0	0.48	5.5	53.3	4.1	1.41	7.66	1.4	0.106	0.85	0.44
890	154.09	0.47	9.2	44.44	4.3	1.15	10.52	1.9	0.183	1.21	0.51
900	155.18	0.33	9.2	38.81	4.1	0.7	6.42	1.19	0.127	0.76	0.30

Table A1. (continued)

Depth, cm	Age, kyr	DBD, g cm ⁻³	SR, cm kyr ⁻¹	Detrital, wt%	Quartz, wt%	MS cm ⁻³ , c.g.s. 10 ⁻⁶	MS, flux	Detrital, flux	Quartz, flux	Feldspar, flux	Other Detr., flux
910	156.27	0.43	9.2	42.39	3.9	0.59	5.36	1.66	0.153	1.05	0.45
920	157.36	0.41	9.2	45.33	3.7	0.81	7.37	1.72	0.143	1.07	0.50
930	158.45	0.44	9.2	50.34	3.7	0.81	7.37	2.03	0.151	1.24	0.64
940	159.54	0.43	9.2	46.74		0.78	7.17	1.83			
950	160.63	0.44	9.2	48.61		0.73	6.71	1.96			
960	161.72	0.49	9.2	59.55		1.03	9.4	2.69			
970	162.81	0.45	9.2	43.4		0.82	7.49	1.80			
980	163.90	0.49	9.2	42.72		0.60	5.48	1.93			
990	165.0	0.44	9.2	39.34		0.67	6.16	1.59			
1000	167.5	0.49	4	42.71		0.66	2.64	0.84			
1010	170.0	0.47	4	57.17		0.89	3.56	1.07			
1020	172.5	0.47	4	52.57		0.88	3.52	0.98			
1030	175.0	0.45	4	42.89		0.77	3.08	0.78			
1040	179.02	0.47	2.5	52.23		0.73	1.82	0.61			
1050	183.03	0.47	2.5	55.23		0.80	1.98	0.64			
1060	184.19	0.47	8.6	47.99		0.76	6.52	1.93			
1070	185.35	0.47	8.6	43.33		0.59	5.04	1.74			
1080	186.52	0.4	8.6	40.73		0.31	2.63	1.4			
1090	187.68	0.43	8.6	33.23		0.20	1.68	1.22			
1100	188.83	0.43	8.6	39.53		0.31	2.63	1.45			
1110	190.0	0.4	8.6	34.86		0.31	2.63	1.2			
1120	191.5	0.45	8.6	22.76		0.21	1.38	0.69			
1130	193.0	0.55	8.6	16.03		0.11	0.73	0.58			
1140	195.0	0.61	5	33.36		0.16	0.79	1.02			
1150	197.0	0.52	5	33.56		0.16	0.79	0.87			
1160	199.0	0.41	5	32.83		0.20	0.98	0.68			
1170	201.0	0.43	5	18.47		0.14	0.68	0.39			

DBD: Dry Bulk Density; SR: Sedimentation Rate; MS: Magnetic Susceptibility; MS flux are expressed in c.g.s. 10⁻⁶ cm⁻² kyr⁻¹; Detrital flux, Quartz flux, Feldspar flux, and Other Detrital flux are expressed in g cm⁻² kyr⁻¹.

Acknowledgments. We sincerely thank T. Corrège and R. Mortlock for discussion and for a helpful review. We thank Denis Kent who provided the low-field magnetic susceptibility record and samples of the Lamont-Doherty Earth Observatory core RC11-120. Piston cores were recovered during the APSARA 4 cruise: we are most grateful to the officers and crew of the R/V Marion-Dufresne. We thank M. Loubet for access to the Finnigan Mat-261 mass spectrometer at the Laboratoire de Géochimie Isotopique (Toulouse, France) and J.L. Joron (CEA-Saclay, France), who helped us with trace-element analyses by neutronic activation. Magnetic susceptibility was measured with a device developed at CFR (Gif-sur-Yvette, France) by F. Guichard and René Manganne. The APSARA IV cruise was funded by the Territoires et Terres Australes et Antarctiques Françaises (TAAF). This work was supported by funds from CNRS-INSU French programs PNEDC.

References

- Alloway, B.V., R.B. Stewart, V.E. Neal, and C.V. Vucetich, Climate of the last glaciation in New-Zealand, based on aerosol quartz influx in an andesitic terrain, *Quat. Res.*, **38**, 170-179, 1992.
- Bareille, G., Flux sédimentaires: Paleoproductivité et Paléocirculation de l'Océan Austral au cours des 150.000 dernières années, thèse de Doctorat, 604, 226 pp., Univ. de Bordeaux I, France, 1991.
- Bareille, G., Labracherie M., Maillet N., and C. Latouche, Quantification des teneurs en opale biogène des sédiments de l'Océan Austral par diffractométrie X. *Clay Miner.*, **25**, 363-373, 1990.
- Bareille, G., M. Labracherie, L.D. Labeyrie, J.J. Pichon, and J.L. Turon, Biogenic silica accumulation rate during the Holocene in the southeastern Indian Ocean, *Mar. Chem.*, **35**, 537-551, 1991.
- Barron, J., et al., *Proceedings of the Ocean Drilling Program, Initial Reports*, vol. 119, College Station, Tex., 1989.
- Biscaye, P.E., Mineralogy and sedimentation of recent deep-sea clay in the Atlantic Ocean and adjacent seas and oceans, *Geol. Soc. Am. Bull.*, **76**, 803-832, 1965.
- Biscaye, P.E., and E.J. Dasch, The rubidium, strontium, strontium isotope system in deep-sea sediments: Argentine Basin, *J. Geophys. Res.*, **76**, 5087-5096, 1971.
- Bloemendal, J., B. Lamb, and J. King, Paleoenvironmental implications of rock-magnetic properties of late Quaternary sediment cores from the eastern equatorial Atlantic, *Paleoceanography*, **3**, 61-87, 1988.
- Bloemendal, J., and P. De Menocal, Evidence for a shift in the climatic variability of the African and Asian monsoons at 2.5Ma: An application of whole-core magnetic susceptibility measurements to palaeoclimatology, *Nature*, **342**, 897-900, 1989.
- Bond, G., H. Heinrich, S. Huon, W. Broecker, L. Labeyrie, J. Andrews, J. McManus, S. Clasen, K. Tedesco, R. Jantschik, C. Simet, and M. Klas, Evidence for massive discharges of icebergs into the glacial Northern Atlantic, *Nature*, **360**, 245-249, 1992.
- Burckle, L.H., D.B. Clarke, and N.J. Shackleton, Isochronous last abundance appearance datum (LAAD) of the diatom *Hemidiscus karstenii* in the sub-Antarctic, *Geology*, **6**, 243-246, 1978.
- Charles, C.D., and R.G. Fairbanks, Evidence from southern ocean sediments for the effect of North Atlantic deep-water flux on climate, *Nature*, **355**, 416-419, 1992.
- Chapuy, B., Les smectites des sédiments marins Quaternaires du Plateau de Kerguelen-Heard (Océan Austral): Nature et origines. Relation avec l'environnement volcanique des îles Kerguelen, littoral et marin, thèse de 3ème cycle, 221 pp., Univ. de Bordeaux I, France, 1988.
- Clemens, S.C., and W.L. Prell, Late pleistocene variability of Arabian sea summer monsoon winds and continental aridity: Aeolian records from lithogenic component of deep-sea sediments, *Paleoceanography*, **5**, 109-145, 1990.

- Cooke, D.W., Variations in the seasonal extent of sea ice in the Antarctic during the last 140,000 years, Ph.D. thesis, Columbia Univ., Palisades, N. Y., 1978.
- Cooke, D.W., and J.D. Hays, Estimates of Antarctic Ocean seasonal sea ice during glacial interval, in *Antarctic Geoscience*, edited by C. Craddock, pp. 1017-1026, University of Wisconsin Press, Madison, 1982.
- Corliss, B.H., Quaternary Antarctic bottom-water history: deep-sea benthonic foraminiferal evidence from the southeast Indian Ocean, *Quat. Res.*, 12, 271-289, 1979.
- Dasch, E.J., Strontium isotopes in weathering profiles, deep-sea sediments and sedimentary rocks, *Geochim. Cosmochim. Acta*, 33, 1521-1552, 1969.
- De Angelis, M., N.I. Barkov, and V.N. Petrov, Aerosol concentrations over the last climatic cycle [160 kyr] from an Antarctic ice core, *Nature*, 325, 318-321, 1987.
- DeMenocal, P., J. Bloemendal, and J. King, A rockmagnetic record of monsoonal dust deposition to the Arabian sea: Evidence for a shift in the mode of deposition at 2.4 Ma., *Proc. Ocean Drill. Program Sci. Results*, 117, 389-401, 1991.
- De Paolo, D.J., W.I. Manton, E.S. Grew, and M. Halpern, Sm-Nd, Rb-Sr and U-Th-Pb systematics of granulite facies rocks from Fyfe Hills, Enderby Land, Antarctica, *Nature*, 298, 614-618, 1982.
- Dosso, L., P. Vidal, J.M. Cantagrel, J. Lameyre, A. Marot, and S. Zimine, "Kerguelen: continental fragment or oceanic island?": Petrology and isotopic geochemistry evidence, *Earth Planet. Sci. Lett.*, 43, 46-60, 1979.
- Dosso, L., H. Bougault, P. Beuzart, J.V. Calvez, and J.L. Joron, The geochemical structure of the South East Indian Ridge, *Earth Planet. Sci. Lett.*, 88, 47-59, 1988.
- Duce, R.A., et al., The atmospheric input of trace species to the world ocean, *Global Biogeochem. Cycles*, 5, 193-260, 1991.
- Duplessy, J.C., N.J. Shackleton, R.G. Fairbanks, L.D. Labeyrie, D. Oppo, and N. Kallel, Deep-water source variations during the last climatic and their impact on global deep-water circulation, *Paleoceanography*, 3, 343-360, 1988.
- Eitrem, S., P.M. Bruchhausen, and M. Ewing, Vertical distribution of turbidity in the South Indian and South Australian Basins, *Antarct. Res. Ser.*, 19, 51-58, 1972a.
- Eitrem, S., A.L. Gordon, M. Ewing, E.M. Thorndike, and P.M. Bruchhausen, The nepheloid layer and observed bottom currents in the Indian-Pacific Antarctic Sea, in *Studies in Physical Oceanography*, edited by A. Gordon, pp. 19-35, New York, 1972b.
- Elderfield, H., C.J. Hawkesworth, and M.J. Greaves, Rare earth element geochemistry of oceanic ferromanganese nodules and associated sediments, *Geochim. Cosmochim. Acta*, 45, 513-528, 1981.
- Erhmann, W.U., and H. Grobe, Cyclic Sedimentation at Sites 745 and 746, *Proc. Ocean Drill. Program Initial Rep.*, 119, 225-235, 1991.
- Erhmann, W.U., M. Melles, G. Kuhn, and H. Grobe, Significance of clay mineral assemblages in the Antarctic Ocean, *Mar. Geol.*, 107, 249-273, 1992.
- Fairbanks, R.G., A 17,000-year glacio-eustatic sea level record: Influence of glacial melting rates on the Younger Dryas event and deep-ocean circulation, *Nature*, 342, 637-642, 1989.
- Faure, G., L.M. Jones, R. Eastin, and M. Christner, Sr isotope composition and trace element concentrations in lake Huron and its principal tributaries, *Rep. 2*, 109 pp., Lab. for Isotope Geol. and Geochem., Ohio State Univ., Columbus, 1967.
- Foldvik, A., T. Gammelsrød, and T. Tørresen, Circulation and water masses on the southern Weddell Sea Shelf, *Antarct. Res. Ser.*, 43, 5-20, 1985.
- Foster, T.D., and J.H. Middleton, Variability in the bottom water of the Weddell Sea, *Deep Sea Res., Part A*, 26, 743-762, 1979.
- Foster, T.D., A. Foldvik, and J.H. Middleton, Mixing and bottom water formation in the shelf break region of the southern Weddell Sea, *Deep Sea Res., Part A*, 34, 1771-1794, 1987.
- Füterer, D.K., H. Grobe, and S. Grünig, Quaternary sediment patterns in the Weddell Sea: Relations and environmental conditions, *Paleoceanography*, 3, 551-561, 1988.
- Gaudichet, A., J.R. Petit, R. Lefèvre, and C. Lorius, An investigation by analytical transmission electron microscopy of individual insoluble microparticules from Antarctic (Dome C) ice core samples, *Tellus*, 38, 250-261, 1986.
- Gaudichet, A., M. De Angelis, R. Lefèvre, J.R. Petit, Y.S. Korotkevich, and V.N. Petrov, Mineralogy of insoluble particules in the Vostok Antarctic ice core over the last climatic cycle (150kyr), *Geophys. Res. Lett.*, 15(13), 1471-1474, 1988.
- Gordon, A.L., Deep Antarctic convection west of Maud Rise, *J. Phys. Oceanogr.*, 8, 600-612, 1978.
- Gordon, A.L., Weddell Deep Water variability, *J. Mar. Res.*, 40, Suppl., 199-217, 1982.
- Gordon, A.L., and E. Molinelli, *U.S.N.S. Eltanin Southern Ocean Oceanographic Atlas*, Lamont-Doherty Geological Observatory, Palisades, N. Y., 1975.
- Gordon, A.L., and B.A. Huber, Thermohaline stratification below the southern ocean sea ice, *J. Geophys. Res.*, 89, 641-648, 1984.
- Griffin, J.J., H. Windom, and E.D. Goldberg, The distribution of clay minerals in the world ocean, *Deep-Sea Res., Part A*, 15, 433-459, 1968.
- Grousset, F.E., J.L. Joron, and M. Treuil, Identification des sources des sédiments quaternaires de la dorsale médio-Atlantique (Islande-Açôres), à l'aide de la géochimie des éléments de transition et des éléments hygromagmaphiles, Coll. Inter. CNRS, Sept. 1981, Bordeaux (France), *Bull. Inst. Géol. du Bassin d'Aquitaine*, 31, 239-256, 1982.
- Grousset, F.E., C. Latouche, and N. Maillet, Clay minerals as indicators of wind and current contribution to post-glacial sedimentation on the Azores/Iceland ridge, *Clay Min.*, 18, 65-75, 1983.
- Grousset, F.E., and R. Chesselet, The Holocene sedimentary regime in the northern Mid-Atlantic Ridge region, *Earth Planet. Sci. Lett.*, 78, 271-287, 1986.
- Grousset, F.E., P.E. Biscaye, A. Zindler, J. Prospero, and R. Chester, Neodymium isotopes as tracers in marine sediments and aerosols, *Earth Planet. Sci. Lett.*, 87, 367-378, 1988.
- Grousset, F.E., F. Henri, J.F. Minster, and A. Monaco, Nd isotopes as tracers in water column particules: The western Mediterranean Sea, *Mar. Chem.*, 30, 389-407, 1990.
- Grousset, F.E., P.E. Biscaye, M. Revel, J.-R. Petit, K. Pye, S. Jousaume, and J. Jouzel, Antarctic (Dome C) ice core dust at 18Ky B.P.: Isotopic constraints on origins, *Earth Planet. Sci. Lett.*, 111, 175-182, 1992.
- Grousset, F. E., L.D. Labeyrie, J.A. Sinko, M. Cremer, G. Bond, J. Duprat, E. Cortijo, and S. Huon, Patterns of ice-rafted detritus in the glacial North-Atlantic (40-55°N), *Paleoceanography*, 8, 175-192, 1993.
- Hampton, M.A., J.H. Kravitz, and G. Luepke, Geology of Sediment Cores from the George V Continental Margin, Antarctica, in *The Antarctic Continental Margin: Geology and Geophysics of Offshore Wilkes Land*, CPCEMR Earth Sci. Ser., vol. 5A, edited by S.L. Eitrem and M.A. Hampton, Circum-Pacific Council for Energy and Mineral Resources, Houston, Tex., 1987.
- Hawkesworth, C.J., R.K. O'Nions, R.J. Pankhurst, P.J. Hamilton, and N.M. Evensen, A geochemical study of island arc and back-arc tholeiites from the Scotia Sea, *Earth Planet. Sci. Lett.*, 36, 253-262, 1977.
- Hays, J.D., J. A. Lozano, N. Shackleton, and G. Irving, Reconstruction of the Atlantic and Western Indian Ocean sectors of the 18,000 B.P. Antarctic Ocean, in *Investigation of Late Quaternary Paleoclimatology and Paleoclimatology*, edited by R.M. Cline and J.D. Hays, Mem. Geol. Soc. Am., 145, 337-372, 1976.
- Heinrich, H., Origin and consequences of cyclic ice rafting in the Northeast Atlantic Ocean during the past 130,000 Years, *Quat. Res.*, 29, 142-152, 1988.

- Heider, F., U. Körner, and P. Bitschene, Volcanic ash particles as carriers of remanent magnetization in deep-sea sediments from the Kerguelen Plateau, *Earth Planet. Sci. Lett.*, **118**, 121-134, 1993.
- Houtz, R.E., D.E. Hayes, and R.G. Markl, Kerguelen Plateau bathymetry, sediment distribution and crustal structure, *Mar. Geol.*, **25**, 95-130, 1977.
- Hovan, S.A., D.K. Rea, N.G. Pisias, and N.J. Shackleton, A direct link between the China loess and marine $\delta^{18}\text{O}$ records: Aeolian flux to the north Pacific, *Nature*, **340**, 296-298, 1989.
- Howard, W.R., and W.L. Prell, Late Quaternary surface circulation of the southern Indian Ocean and its relationship to orbital variations, *Paleoceanography*, **7**, 79-117, 1992.
- Imbrie, J., J.D. Hays, D.G. Martinson, A. McIntyre, A.C. Mix, J.J. Morley, N.G. Pisias, W.L. Prell, and N.J. Shackleton, The orbital theory of Pleistocene climate: Support from a revised chronology of the marine ^{18}O record, in *Milankovič and Climate*, edited by A.L. Berger, J. Imbrie, J.D. Hays, G.J. Kukla, and B. Saltzman, pp. 269-277, Reidel, Norwell, Mass., 1984.
- Jacobs, S.S., A.F. Amos, and P.M. Bruchhausen, Ross Sea oceanography and Antarctic Bottom Water formation, *Deep Sea Res., Part A*, **17**, 935-962, 1970.
- Jacobs, S.S., The voyage of Iceberg B-9, *Am. Sci.*, **80**, 32-42, 1992.
- Keir, R., On the late Pleistocene ocean geochemistry and circulation, *Paleoceanography*, **3**, 443-445, 1988.
- Kennett, J.P., and N.D. Watkins, Deep-sea erosion and manganese nodule development in the southeast Indian Ocean, *Science*, **188**, 1011-1013, 1975.
- Kennett, J.P., and N.D. Watkins, Regional deep-sea dynamic processes recorded by late Cenozoic sediments in the southeastern Indian Ocean, *Geol. Soc. Am. Bull.*, **87**, 321-339, 1976.
- Kent, D.V., Apparent correlation of palaeomagnetic intensity and climatic records in deep-sea sediments, *Nature*, **299**, 538-539, 1982.
- Killworth, P.D., On "chimney" formations in the ocean, *J. Phys. Oceanogr.*, **9**, 531-554, 1979.
- Klinck, J.M., and D.A. Smith, Effect of wind changes during the last glacial maximum on the circulation in the southern ocean, *Paleoceanography*, **8**, 427-433, 1993.
- Kolla, V., and P.E. Biscaye, Distribution and origin of quartz in the sediments of the Indian Ocean, *J. Sediment. Petrol.*, **47**, 642-649, 1976.
- Kolla, V., L. Henderson, and P.E. Biscaye, Clay mineralogy and sedimentation in the western Indian ocean, *Deep Sea Res.*, **23**, 949-961, 1976.
- Kolla, V., L. Sullivan, S.S. Streeter, and M.G. Langseth, Jr., Spreading of Antarctic Bottom Water and its effects on the floor of the Indian Ocean inferred from bottom-water potential temperature, turbidity, and sea-floor photography, *Mar. geol.*, **21**, 171-189, 1976.
- Kolla, V., L. Henderson, L. Sullivan, and P.E. Biscaye, Recent sedimentation in the southeast Indian Ocean with special reference to the effects of Antarctic bottom water circulation, *Mar. geol.*, **27**, 1-17, 1978.
- Kukla, G., Loess stratigraphy in central China, *Quat. Sci. Rev.*, **6**, 191-219, 1987.
- Kukla, G., and Z. Han, Loess stratigraphy in central China, *Paleogeogr. Paleoclimatol. Paleoecol.*, **72**, 203-225, 1989.
- Kukla, G., F. Heller, L.X. Ming, X.T. Sheng, and A.Z. Sheng, Pleistocene climates in China dated by magnetic susceptibility, *Geology*, **16**, 811-814, 1988.
- Labeyrie, L.D., J.J. Pichon, M. Labracherie, P. Ippolito, J. Duprat, and J.C. Duplessy, Melting history of Antarctica during the past 60,000 years, *Nature*, **322**, 701-706, 1986.
- Labeyrie L.D., J.C. Duplessy, and P.L. Blanc, Variations in mode of formation and temperature of oceanic deep waters over the past 125,000 years, *Nature*, **327**, 477-482, 1987.
- Labracherie, M., L.D. Labeyrie, J. Duprat, E. Bard, M. Arnold, J.J. Pichon, and J.C. Duplessy, The last deglaciation in the Southern Ocean, *Paleoceanography*, **4**, 629-638, 1989.
- Martinson, D.G., N.G. Pisias, J.D. Hays, J. Imbrie, T.C. Moore, and N.J. Shackleton, Age dating the orbital theory of the Ices Ages: Development of a high-resolution 0 to 300,000-years chronostratigraphy, *Quat. Res.*, **27**, 1-29, 1987.
- Morche, W., H.-W. Hubberten, W.U. Ehrmann, and J. Keller, Geochemical investigations of volcanic ash layers from Leg 119, Kerguelen Plateau, *Proc. Ocean Drill. Program Initial Rep.*, **119**, 323-344, 1991.
- Mortlock, R.A., and P.N. Froelich, A simple method for the rapid determination of biogenic opal in pelagic marine sediments, *Deep Sea Res.*, **36**, 1415-1426, 1989.
- Mortlock, R.A., C.D. Charles, M.A. Zibello, P. Malone, J. Saltzman, C. Wang, J.D. Hays, L.H. Burckle, and P.N. Froelich, Reduced productivity in the Antarctic Ocean during the last glacial, *Nature*, **351**, 220-223, 1991.
- Mounier, L., Etude des microparticules insolubles déposées dans la glace Antarctique au cours du dernier cycle climatique, thèse de Doctorat, 179 pp., Univ. of Grenoble, Grenoble, France, 1988.
- Nowlin, W.D., On water mass exchange between the Southern Ocean and the World Ocean: Emphasis on the Atlantic sector, *Mar. Chem.*, **35**, 1-7, 1991.
- Nowlin, W.D., and J.M. Klinck, The physics of the Antarctic Circumpolar Current, *Rev. Geophys.*, **24**, 469-491, 1986.
- O'Nions, R.K., and R.J. Pankhurst, Petrogenetic significance of isotope and trace element variations in volcanic rocks from the Mid-Atlantic Ridge, *J. Petrol.*, **15**, 603, 1974.
- Palmer, M.R., Rare earth elements in foraminifera tests, *Earth Planet. Sci. Lett.*, **73**, 285-298, 1985.
- Petit, J.R., M. Briat, and A. Royer, Ice age aerosol content from East Antarctic ice core samples and past wind strength, *Nature*, **293**, 391-394, 1981.
- Petit, J.R., L. Mounier, J. Jouzel, Y.S. Korotkevich, V.I. Kotlyakov, and C. Lorius, Palaeoclimatological and chronological implications of the Vostok core dust record, *Nature*, **343**, 56-58, 1990.
- Pichon, J.J., L.D. Labeyrie, G. Bareille, M. Labracherie, J. Duprat, and J. Jouzel, Surface water temperature changes in the high latitudes of the southern hemisphere over the last glacial-interglacial cycle, *Paleoceanography*, **7**, 289-318, 1992.
- Poutiers, J., Sur les propriétés magnétiques de certains sédiments continentaux et marins: Applications, thèse de doctorat, 492, 266 pp., Univ. Bordeaux I, France, 1975.
- Poutiers, J., and E. Gonthier, Sur la susceptibilité magnétique des sédiments du bassin d'Islande comme indicateur de la dispersion du matériel volcanoclastique à partir de l'Islande et des Faerø (mission Faegas 2), *Bull. Inst. de Géol. du Bassin Aquitaine*, **23**, 214-226, 1978.
- Pudsey, C.J., Late Quaternary changes in Antarctic Bottom Water velocity inferred from sediment grain size in the northern Weddell Sea, *Mar. Geol.*, **107**, 9-33, 1992.
- Pudsey, C.J., P.F. Barker, and N. Hamilton, Weddell Sea abyssal sediments: a record of Antarctic bottom water flow, *Mar. geol.*, **81**, 289-314, 1988.
- Rea, D.K., Aspects of atmospheric circulation: The late Pleistocene (0-950,000 yr) record of eolian deposition in the Pacific Ocean, *Paleogeogr. Paleoclimatol. Paleoecol.*, **78**, 217-228, 1990.
- Rea, D.K., L.W. Chambers, J.M. Chuey, T.M. Janecek, M. Leinen, and N.G. Pisias, A 420,000-year record of cyclicity in oceanic and atmospheric processes from the eastern equatorial Pacific, *Paleoceanography*, **1**, 577-586, 1986.
- Robinson, S.G., The late Pleistocene palaeoclimatic record of North Atlantic deep-sea sediments revealed by mineral-magnetic measurements, *Phys. Earth Planet. Int.*, **42**, 22-47, 1986a.
- Robinson, S.G., Mineral magnetism of deep-sea sediments: Paleoclimatic implications, Ph.D. thesis, Univ. Liverpool, United Kingdom, 1986b.
- Ruhlin, D.E., and R.M. Owen, The rare earth element geochemistry of hydrothermal sediments from the East Pacific Rise: Examination of a

- seawater scavenging mechanism, *Geochim. Cosmochim. Acta*, 50, 393-400, 1985.
- Sarnthein, M.G., G. Tetzlaff, B. Koopmann, K. Wolter, and U. Pflaumann, Glacial and interglacial wind regimes over eastern subtropical Atlantic and north-west Africa, *Nature*, 293, 193-293, 1981.
- Thiede, J., Wind regimes over the late Quaternary southwest Pacific Ocean, *Geology*, 7, 259-262, 1979.
- Toggweiler, R., and J. Sarmiento, Glacial to Interglacial changes in the atmospheric carbon dioxide: The critical role of the surface water in high latitudes, in *The Carbon Cycle and Atmospheric CO₂: Natural variations Archean to Present*, *Geophys. Monogr. Ser.*, vol. 32, edited by E. Sundquist and W. Broecker, pp. 99-110, AGU, Washington, D.C., 1985.
- Wenk, T., and U. Siegenthaler, The high latitude ocean control of atmospheric CO₂, in *The Carbon Cycle and Atmospheric CO₂: Natural variations Archean to Present*, *Geophys. Monogr. Ser.*, vol. 32, edited by E. Sundquist and W. Broecker, pp. 185-194, AGU, Washington, D.C., 1985.
- Zindler, A., E. Jagoutz, and S.L. Goldstein, Nd, Sr and Pb systematics in a three component mantle, *Nature*, 298, 519-523, 1982.
-
- G. Bareille, F. E. Grousset, and M. Labracherie, Departement de Geologie et Oceanographie, CNRS-URA 197, Universite de Bordeaux I, Avenue des Facultés, 33405 Talence, France.
- L. D. Labeyrie, Centre des Faibles Radioactivites, Laboratoire mixte CNRS-CEA, Avenue de la Terrasse, 91198 Gif-sur-Yvette, France.
- J.-R. Petit, Laboratoire de Glaciologie et Géophysique de l'Environnement, BP 96, 38402 St Martin-d'Heres, France.

(Received March 28 1994; revised July 24 1994;
accepted July 26, 1994.)